KTH Land and Water
Resources Engineering

A MULTI-RESOLUTION APPROACH FOR MODELING FLOW AND SOLUTE TRANSPORT IN HETEROGENEOUS POROUS MEDIA

Hrvoje Gotovac

June 2009

TRITA-LWR PhD Thesis 1051
ISSN 1650-8602
ISRN KTH/LWR/PHD 1051-SE
ISBN 978-91-7415-377-4

Doctoral Thesis
KTH-International Groundwater Arsenic Research Group
Department of Land and Water Resources Engineering
Royal Institute of Technology (KTH)
SE-100 44 STOCKHOLM, Sweden
E-mail: gotovac@kth.se

Department of Civil and Architectural Engineering
University of Split
21000 SPLIT, Croatia
E-mail: hrvoje.gotovac@gradst.hr

DEDICATION

This thesis is dedicated to my family…

"Uspjeh neke ideje u praksi, neovisno o njenim unutarnjim kvalitetama, ovisi o tome kakav stav prema njoj imaju suvremenici. Ako se pojavi u pravo vrijeme, ljudi je brzo prihvate; ako ne, tada je kao mladicu biljke toplina sunca namami iz tla samo s jednim ciljem – da je prvi mraz ozlijedi i uspori joj rast."

"The practical success of an idea, irrespective of its inherent merit, is dependent on the attitude of the contemporaries. If timely it is quickly adopted; if not, it is apt to fare like a sprout lured out of the ground by warm sunshine, only to be injured and retarded in its growth by the succeeding frost."

Nikola Tesla

FLERSKALIG UPPLÖSNINGSMETODIK FÖR MODELLERING AV VATTENFLÖDE OCH ÄMNESTRANSPORT I HETEROGENA PORÖSA MEDIER

Markprocesser karakteriseras ofta av fåtaliga fältexperiment, glesa mätningar, heterogenitet på olika skalor, slumpmässighet och relaterade osäkerheter, samt beräkningsmässiga svårigheter. Under de senaste årtiondena har olika beräkningstekniker och strategier blivit ovärderliga verktyg för att förutspå vattenflöde och ämnestransport i heterogena porösa medier. Denna doktorsavhandling utvecklar ett angreppssätt med flerskaliga upplösningar baserat på Fup basis funktioner med kompakt stöd, som möjliggör en effektiv och anpassningsbar procedur, nära relaterad till rådande fysiska tolkningar. Alla flödes- och transportvariabler, så väl som heterogeniteten, beskrivs av en flerskaligt upplöst representation, i form av linjära kombinationer av Fup basis funktioner. Varje variabel representeras på ett speciellt anpassningsbar gridnät med given noggrannhet. Metoden appliceras för att lösa problem med skarpa fronter, samt vattenflöde och advektiv ämnestransport i starkt heterogena porösa medier. Adaptive Fup collocation metoden tillsammans med den välkända *Method of lines*, spårar effektivt lösningar med skarpa fronter och löser upp positioner och frekvenser på alla rums- och/eller tidsskalor. Metoden ger kontinuerliga hastighetsfält och flöden, och möjliggör noggrann och tillförlitlig transportanalys. Analys av advektiv transport understöder stabiliteten i första-ordningens transport teori för låg och mild heterogenitet. Utöver detta, som resultat av noggrannheten i den förbättrade Monte-Carlo metodiken, visar denna avhandling effekten av hög heterogenitet på ensemble statistiken för flöden och transporttider. Skillnaden mellan Eulerisk och Lagrangian hastighetsstatistik och betydelsen av högre statistiska moment för transporttider, indikerar hög heterogenitet. Det tredje transporttidsmomentet beskriver huvudsakligen sannolikhetspiken och de långa transporttiderna, medan högre moment behövs för de korta transporttiderna, som har den största osäkerheten. En speciell upptäckt är linjäariteten i transporttidsmoment, som indikerar att advektiv transport i multi-Gaussiska fält blir Gaussisk i gränsen. Som jämförelse konvergerar sannolikhetsfunktioner för den transversella transportförflyttningen mot en Gaussisk fördelning vid runt 20 korrelationslängder efter injektion, även för hög heterogenitet. Förmågan i det presenterade angreppssättet med flerskalig upplösning, och resultatens noggrannhet, öppnar nya områden för fortsatt forskning.

Nyckelord: Flerskalig upplösning; anpassningsbar upplösning; Atomic och Fup basis Funktioner; Monte Carlo metod; heterogena porösa medier; grundvatten flöde; advektiv transport; transporttider.

VIŠE-REZOLUCIJSKI PRISTUP ZA MODELIRANJE TOKA I PRONOSA U HETEROGENOJ POROZNOJ SREDINI

Procesi toka i pronosa u podzemlju obično su karakterizirani nedostatkom mjerenja, njihovim više-rezolucijskim i stohastičkim opisom te pripadajućom nepouzdanošću i kompleksnom analizom. Posljednjih su nekoliko desetljeća različite računalne tehnike i metode postale nezaobilazni alati za predviđanje i analizu procesa toka i pronosa u heterogenim poroznim sredinama. U ovoj je tezi razvijen više-rezolucijski pristup temeljen na Fup baznim funkcijama s kompaktnim nosačem, koji omogućava efikasnu i adaptivnu proceduru blisku trenutačno poznatoj fizikalnoj interpretaciji podzemnih procesa. Varijable toka i pronosa u podzemlju opisane su na više-rezolucijski način u obliku linearne kombinacije Fup baznih funkcija, pri čemu svaka varijabla ima zaseban adaptivni grid (raspored kolokacijskih točaka) i pripadajuću točnost. Razvijena metodologija primijenjena je u podzemnim procesima, čija su rješenja određena oštrim frontovima, te u rješavanju toka i advektivnog pronosa u izrazito heterogenim Gaussovim sredinama uslijed jednolikog srednjeg toka. Adaptivna Fup kolokacijska metoda, koristeći dobro poznati koncept linija, efikasno prati dinamiku frontova na adaptivnom gridu, koji pokazuje položaj i frekvencije svih prostornih i vremenskih skala. Procedura daje kontinuirana polja brzina i flukseva omogućavajući točnu i pouzdanu analizu pronosa. Analiza advektivnog pronosa još jedanput dokazuje kvalitetu teorije prvog reda za male i srednje heterogenosti kod kojih je sve opisano s prva dva statistička momenta. Međutim, zbog točnosti poboljšane Monte-Carlo metode dane u ovoj tezi, analizirani su efekti visoke heterogenosti na statistiku toka i pronosa u podzemlju. Razlika između Eulerove i Lagrangeove brzine te utjecaj viših momenata vremena putovanja u podzemlju indikatori su visoke heterogenosti. Treći moment opisuje maksimum i zadnje dolaske funkcije gustoće vjerojatnosti vremena putovanja, dok viši momenti uglavnom opisuju prve dolaske koji su suočeni s najvećom nepouzdanošću, a imaju ključni utjecaj u analizi rizika i regulative o vodama. Prikazana analiza otkriva da su svi momenti vremena putovanja linearni, što implicira da advektivni pronos konvergira u klasičan Fickov pronos. S druge strane, funkcija gustoće vjerojatnosti transverzalnog pomaka konvergira u Gaussovu razdiobu već nakon dvadeset korelacijskih duljina nakon utiskivanja, čak i za velike heterogenosti. Svojstva i mogućnosti prikazanog više-rezolucijskog pristupa te kvaliteta i točnost dobivenih rezultata otvaraju nove mogućnosti i smjernice za daljnja istraživanja u podzemlju.

Ključne riječi: Više-rezolucijski adaptivni pristup, Atomske i Fup bazne funkcije; Monte-Carlo metoda; Heterogene porozne sredine; Tok; Pronos; Vrijeme putovanja.

ACKNOWLEDGMENTS

I would like to particularly thank three people who had important scientific roles during my work on this thesis. First, I want to thank my advisor, Professor Vladimir Cvetković at the Department of Land and Water Resources Engineering, KTH, for his support and scientific guidance. I appreciate his spirit and enthusiasm, which allowed me freedom and space for creativity. Furthermore, he helped in each critical moment during this work, as a Professor, but also as a friend. I also thank my co-advisor, Professor Roko Andričević at the Department of Civil and Architectural Engineering, University of Split, for his support, encouragement and vision. He accepted me as a researcher and believed in me from the beginning. I really appreciate that he inspired me with stochastic modeling and heterogeneity. Finally, I would like to thank Blaž Gotovac for his dual role as both father and Professor. Apart from his knowledge and experience in atomic basis functions and numerical analysis, our many discussions and debates formed my personality as a man and as a scientist. I could not have imagined that Fup basis functions would become a part of our family tradition.

I want to thank all of the staff and Ph.D. students at LWR-KTH and GAF-Split for their company, understanding, interesting discussions and help. I am particularly grateful to Staffan Molin, KTH, for inspiring discussions and friendship; Andrew Frampton, KTH, for valuable help with Linux and review of "Kappa"; and Veljko Srzić from Split, for his help in preparation of the text and presentation. I want to thank the PDC (KTH-NADA) staff for their valuable help during the running of Monte-Carlo simulations on the Lenggren cluster. I also want to thank Professor Georgia Destouni and Carmen Prieto, Stockholm University, for good collaboration in the WASSER project, before this thesis. I am grateful to Aira Saarelainen, for valuable help in administrative matters. Aira always makes these complicated things for a scientist into very easy and relaxing experiences. I want to particularly thank Aleksandra, Carmen, and their families for friendship during my stay here in Stockholm. Finally, yet importantly, I want to thank all of my LWR-KTH colleagues for exciting "innebandy" games and pleasant breaks from the science.

I would like to warmly thank my whole family, especially my wife Korana for her love, understanding and handling of all responsibilities during my work in Stockholm. Dear Korana, this success belongs to both of us! I am particularly grateful to my kids, Nora and Karlo, for their special kind of support. They were permanent inspirations during good and bad times, both in life and in science. Finally, I want to thank my mother, sister and parents-in-law for their support, love and understanding; I do not believe that this thesis would have been possible without them.

Hrvoje Gotovac
Stockholm, May 2009

LIST OF PAPERS

I. Gotovac H, Andričević R, Gotovac B. 2007. Multi – resolution adaptive modeling of groundwater flow and transport problems. *Advances in Water Resources,* 30: 1105-1126.

II. Gotovac H, Cvetković V, Andričević R. 2009. Adaptive Fup multi-resolution approach to flow and advective transport in highly heterogeneous porous media: Methodology, accuracy and convergence. *Advances in Water Resources*, doi:10.1016/j.advwatres.2009.02.013, 32: 885-905.

III. Gotovac H, Cvetković V, Andričević R. 2009. Flow and travel time statistics in highly heterogeneous porous media. *Water Resources Research,* doi:10.1029/2008WR007168, in press.

IV. Gotovac H, Cvetković V, Andričević R. 2009. Significance of higher order moments to the complete characterization of the travel time pdf in heterogeneous porous media using the maximum entropy principle. *Water Resources Research,* in review.

V. Gotovac H, Gotovac B. 2009. Inexact Maximum Entropy algorithm based on Fup basis functions with compact support. *Journal of Computational Physics,* in review.

LIST OF PAPERS, PRESENTATIONS AND REPORTS NOT INCLUDED IN THE THESIS

VI. Gotovac H, Andričević R, Gotovac B, Kozulić V, Vranješ M. 2003. An improved collocation method for solving the Henry problem. *Journal of Contaminant Hydrology*, 64: 129-149.

VII. Kozulić V, Gotovac H, Gotovac B. 2007. An Adaptive Multi-resolution Method for Solving PDE's. *Computers, Materials and Continua*, 6(2): 51-70.

VIII. Gotovac H, Andričević R, Vranješ M. 2001. Effects of aquifer heterogeneity on the intrusion of sea water, Proceedings of The First International Conference on Salt Water Intrusion and Coastal Aquifers, Monitoring, Modeling and Management, Essaouira, Morocco, April 23-25.

IX. Gotovac H, Andričević R, Vranješ M. 2003. Collocation method for solving the saltwater intrusion problems, Proceedings of The Second International Conference on Salt Water Intrusion and Coastal Aquifers, Monitoring, Modeling and Management, Merida – Yucatan, Mexico, March 29-April 2.

X. Gotovac H, Andričević R, Vranješ M, Radelja T. 2005. Multilevel adaptive modeling of multiphase flow in porous media, Proceedings of The Computational Methods in Multiphase Flow III, Portland, Maine, USA, November 2-5.

XI. Andričević R, Gotovac H, Lončar M, Srzić V. 2008. Risk assessment from oil waste disposal in deep wells. Power Point Presentation in Risk analysis VI: Simulation and Hazard Mitigation / Brebbia CA, Popov V, Beriatos E. (Editors). Southampton, UK: WIT Press, May 5-8.

XII. Prieto C, Gotovac H, Berglund S, Destouni G, Andričević R. 2000. Israel case Study: Deterministic and temporal variability investigations, in 2nd WASSER Progress report. Annex I.1, Volume 1, National Observatory of Athens.

XIII. Berglund S, Gotovac H, Destouni G, Andričević R, Prieto C. 2000. Israel case Study: First results of stochastic simulations, in 2nd WASSER Progress report. Annex I.2, Volume 1, National Observatory of Athens.

XIV. Prieto C, Gotovac H, Berglund S, Destouni G, Andričević R. 2001. Final report, in 3rd WASSER Progress report. Annex I.1, Volume 1, National Observatory of Athens.

TABLE OF CONTENTS

ABSTRACT

Subsurface processes are usually characterized by rare field experiments, sparse measurements, multi-resolution interpretations, stochastic description, related uncertainties and computational complexity. Over the last few decades, different computational techniques and strategies have become indispensable tools for flow and solute transport prediction in heterogeneous porous media. This thesis develops a multi-resolution approach based on Fup basis functions with compact support, enabling the use of an efficient and adaptive procedure, closely related to current understood physical interpretation. All flow and transport variables, as well as intrinsic heterogeneity, are described in a multi-resolution representation, in the form of a linear combination of Fup basis functions. Each variable is represented on a particular adaptive grid with a prescribed accuracy. The methodology is applied to solving problems with sharp fronts, and to solving flow and advective transport in highly heterogeneous porous media, under mean uniform flow conditions. The adaptive Fup collocation method, through the well known method of lines, efficiently tracks solutions with sharp fronts, resolving locations and frequencies at all spatial and/or temporal scales. The methodology yields continuous velocity fields and fluxes, enabling accurate and reliable transport analysis. Analysis of the advective transport proves the robustness of the first-order theory for low and mild heterogeneity. Moreover, due to the accuracy of the improved Monte-Carlo methodology, this thesis presents the effects of high heterogeneity on ensemble flow and travel time statistics. The difference between Eulerian and Lagrangian velocity statistics and the importance of higher travel time moments are indicative of high heterogeneity. The third travel time moment mostly describes a peak and late arrivals, while higher moments are required for early arrivals which are linked with the largest uncertainty. A particular finding is the linearity of all travel time moments, which implies that in the limit an advective transport in multi-Gaussian field becomes Fickian. By comparison, the transverse displacement pdf converges to a Gaussian distribution around 20 integral scales after injection, even for high heterogeneity. The capabilities of the presented multi-resolution approach, and the quality of the obtained results, open new areas for further research.

Key words: Multi-resolution adaptive approach; Atomic and Fup basis functions; Monte-Carlo method; Heterogeneous porous media; Flow; Transport; Travel time.

1 INTRODUCTION

This section presents general features of flow and transport in porous media, as well as an overview of numerical and stochastic methods used in subsurface modeling. Moreover, transport concepts, motivations and objectives of the research in this thesis will be presented.

1.1 General features of flow and solute transport in heterogeneous porous media

Flow and solute transport in porous media is covered in the fields of subsurface hydrogeology and hydrology, and presents two important dilemmas: homogeneous vs. heterogeneous porous media, and deterministic vs. stochastic approaches. Geological formations usually exhibit such complex patterns of spatial variability of hydraulic conductivity, porosity and/or other physical and chemical properties that porous media cannot be regarded as homogeneous. Because the available data are usually quite scarce, analysis of flow and transport is never certain and absolutely known in the deterministic sense; so stochastic quantification remains the only rational way to represent uncertainty in predictions of subsurface processes. Therefore, over the past few decades, subsurface hydrogeology and hydrology has primarily developed as an applied science based on stochastic approaches, due to uncertainties in the basic properties, such as hydraulic conductivity, of heterogeneous porous media (Dagan, 1989; Gelhar, 1993; Rubin, 2003).

Uncertainty, as a measure of the stochastic description of subsurface processes, can be divided into two main types: i) intrinsic uncertainty, caused by natural variability in basic physical and chemical properties, and ii) parametric uncertainty, caused by simplifications and assumptions used in conceptual models, or errors in measurements of the model parameters. The latter type of uncertainty can be reduced or even eliminated by employing a more appropriate conceptual model supported by additional, more accurate input data. However, the former uncertainty cannot be reduced. The most attention has been devoted to the representation of the intrinsic variability of hydraulic conductivity as a stochastic random field (SRF).

The hydraulic log-conductivity is usually represented by only three parameters: the mean value, the variance-σ_Y^2 as a measure of spatial variability and the integral scale-I_Y (related to the correlation length) as a measure of spatial connectivity. This representation implies the hypothesis of weak statistical stationarity. Furthermore, the SRF commonly appears as a suitable stochastic concept for representing spatial distributions of random input variables, such as porosity, hydraulic conductivity, sorption, dispersivity, recharge or boundary conditions, while also considering, in a consistent fashion, their influence on random output variables, such as head, velocity, concentration, solute flux, travel time or mass transfer parameters.

Unfortunately, field and laboratory experiments usually do not offer sufficient data for comprehensive analyses of flow and transport. Rare, extensive tracer experiments have been performed in well-known examples of low heterogeneity, the Borden (σ_Y^2=0.29; Mackay et al., 1986) and Cape Cod (σ_Y^2=0.26; LeBlanc et al., 1991) aquifers, and in the highly heterogeneous Columbus aquifer (MADE-1 and MADE-2 tracer test; Boggs et al., 1992) with σ_Y^2 approximately equal to 4.5. Columbus aquifer consists of, for instance, alluvial terrace deposits composed of sand and gravel with minor amounts of silt and clay, and the measured hydraulic conductivity values span over six orders of magnitude.

Moreover, hydraulic and other input properties are defined on many spatial length scales: from pore scale, to some large macro-scale appropriate for defining the macroscopic governing equations such as Darcy's law, Fick's Law, or the advection-dispersion-reaction equation. As a consequence, the previously mentioned input and output flow and transport variables are also defined on different spatial and temporal scales. Furthermore, different measurement techniques consider input variables on different scales; for instance, core laboratory measurements are obtained on scales of 5-10 cm, geoelectric measurements of resistivity or spontaneous potential are on scales of 40-160 cm, flow-meter tests are on the scale of meters, pumping tests are on scales of tens or hundreds of meters, while seismic measurements can capture the influence of very large areas and scales. Some of these measurements present hard (direct) data, but some of them produce soft data (indirect data that can be subjected to other descriptive analyses, such as geologic descriptions, or expert judges). Therefore, the field experiments and physical interpretations of subsurface processes present its inherent multi-scale, or multi-resolution, nature (Rubin, 2003).

Subsurface processes are generally complex, and site characterization through a common geostatistical analysis is required (Kitanidis, 1997). These processes can be divided into a few main groups: i) single-phase flow, and transport of tracers and contaminants where velocity and concentration are decoupled (mainly discussed in this thesis, papers II-IV; Dagan, 1989; Rubin, 2003), ii) flow driven by density, viscosity, or temperature, and miscible transport of salts or contaminants where velocity and concentration are coupled (paper I; Simmons et al, 2001; Diersch and Kolditz, 2002; Gotovac et al., 2003) and iii) multiphase flow or immiscible transport, where the saturation of each phase present in the porous media is of interest (paper I; Helmig, 1998). All three types can encompass non-reactive (conservative, e.g. Bellin et al., 1992) and reactive transport (e.g. Cvetković and

Dagan, 1994a, b). This general separation of flow regimes and their transport counterparts allows different conceptual frameworks and computational methodologies to be used to represent flow and solute transport in heterogeneous porous media. Note that the influence of heterogeneity on the more complex flow regimes, such as density driven or multi-phase flow, is much less understood than the cases of single-phase or tracer flow and transport.

Even in cases in which extensive field tracer experiments have been performed (MADE-1 and MADE-2 tracer test; e.g. Boggs et al., 1992), a computational stochastic description is needed for appropriate physical interpretation and understanding. For instance, MADE tracer tests have been explained by employing a few different conceptual frameworks (e.g. Harvey and Gorelick, 2000). Faced with the usual scarcity of data and complexity of subsurface processes, requirements for novel, more efficient methodologies arise due to practical and theoretical considerations. These methodologies must cover the correct physical interpretation of flow regimes in a simple and comprehensive manner, relate the parameters of the conceptual framework to sparse measurements while respecting their multi-resolution nature, satisfy the requirements of accuracy and convergence and keep the computational burden to an acceptable level.

1.2 Review of numerical and stochastic methods in the subsurface modeling

A review of numerical and stochastic methods is presented, mainly for single-phase flow and solute transport in heterogeneous porous media. The separation of these two methods is rather illustrative. Numerical methods are usually directly linked with stochastic tools, and therefore it is impossible to define a sharp interface between them.

1.2.1 Numerical methods

As in many other fields, conventional methods such as the finite difference (FD), finite element (FE) and finite volume (FV) methods take an important place in subsurface modeling. The flow problem is defined by Darcy's Law

$$\mathbf{q}(\mathbf{x}) = -\mathbf{K}(\mathbf{x})\nabla h(\mathbf{x}) \tag{1}$$

and the continuity equation

$$\nabla \cdot \mathbf{q}(\mathbf{x}) = 0 \tag{2}$$

where $\mathbf{q}$ is the Darcy specific discharge (L/T), $\mathbf{K}$ is the conductivity tensor (L/T) and h (L) is the hydraulic head. Assuming an isotropic log-conductivity field (Y=lnK), the 2-D steady-state flow equation has the final form

$$\frac{\partial^2 h}{\partial x^2} + \frac{\partial^2 h}{\partial y^2} + \frac{\partial Y}{\partial x}\frac{\partial h}{\partial x} + \frac{\partial Y}{\partial y}\frac{\partial h}{\partial y} = 0 \tag{3}$$

subject to the corresponding boundary conditions. Note that it is easy to transform Eq. (3) to state it in terms of the conductivity K. The most widely used flow solver is MODFLOW (McDonald and Harbouch, 1988), based on a 5-point stencil and block-centered FD approximation to Eq. (3). The domain is divided into blocks, each of which has a constant conductivity, which varies from one block to the next. Therefore, the conductivity is represented as the inter-block conductivity in the 5-point stencil, obtained as the harmonic or geometric mean of two adjacent blocks.

The simple "MODFLOW" procedure has become the state of the art for 3-D flow solvers (7 point stencil; Ababou et al., 1989). The procedure is easy to implement and very stable, even in cases with pumping, high heterogeneity and transient calculations. The result of the procedure is a continuous velocity field with constant velocities across the block edges. The numerical implementation reduces the flow problem (3) to a symmetric system of linear equations, which can be efficiently solved by the preconditioned conjugate gradient algorithm. A recent interpretation of this algorithm, in a parallel, 2-D form, was given by de Dreuzy et al. (2007) for simulations with high heterogeneity. The disadvantages of this approach lie in the low-order head and velocity approximations, and the description of irregular geometries.

FE techniques use localized basis functions to discretize Eq. (3) on finite elements with constant conductivity, with the conductivity

varying over the mesh. The solution can describe irregular geometries, but the standard FE scheme suffers from velocity discontinuities along the element edges. This inherent drawback to the FE method can be solved by a velocity postprocessor (Cordes and Kinzelbach, 1992) or with a mixed hybrid FE formulation (e.g. Mose et al., 1994); both cases involve additional CPU work or a higher number of unknowns (velocities in the element edges), significantly detracting from the efficiency and robustness of the FE algorithm. Classical FE solutions for 2-D steady flow for low and mild heterogeneity have been presented by Bellin et al. (1992), and by Salandin and Fiorotto (1998) for high heterogeneity. The USGS software counterpart to MODFLOW is the well-known FE code SUTRA (Voss, 1984). Recently, the FE code FEFLOW (Diersch and Kolditz, 2002) has been developed, which is very powerful and reliable, particularly for density driven flow.

Conventional methods require fine solution scales in order to capture all the effects of heterogeneity. A common approach to overcome these difficulties is to use an upscaling procedure, which finds effective conductivities on a coarse scale in an attempt to solve the macroscopic properties of flow in porous media, defined for all scales (e.g., Kitanidis, 1990, Durlofsky, 1992). Upscaling methods require restrictive assumptions about the heterogeneity (Hou and Wu, 1997).

On the other hand, recent finite-element and other multiscale methods have tried to find fine scale velocity solutions on a coarse grid, using the only most relevant fine scale information (e.g. Enquist et al., 2003). Hou and Wu (1997) and Hou et al. (1999) first presented the multiscale finite element method (MsFEM) for flow in porous media by constructing generalized velocity basis functions on a coarse grid, which satisfy local or fine scale properties of the differential operator. This local solution is not too computationally expensive, and can be found in many ways (e.g. Jenny et al., 2003; Aarnes, 2004). The general methodology of a heterogeneous multiscale method was given by Enquist et al. (2003) and E et al. (2004). Recently, using the multi-scale methodology and the basic principles of Hou and Wu (1997), He and Ren (2005) presented the finite volume multiscale finite element method, where generalized velocity basis functions are implemented in a macro-scale finite volume implementation, for cases with high heterogeneity, pumping and transient calculations.

However, errors in the velocity, due to loss of particular fine scale information, can play a key role for some important features of flow and transport in highly heterogeneous porous media, such as early arrivals, travel time peaks and tailings, asymptotic dispersivity or higher-order moments of solute flux or concentration. Unfortunately, this means that the fine scale velocity field is usually required, which implies the use of extensive CPU resources to extend all aforementioned approaches to 3-D flows.

Rare, extensive, 3-D flow numerical simulations in heterogeneous porous media have been performed with the analytic element method (AEM; Strack, 1989; Janković and Barnes, 1999; Janković et al., 2003, 2006), using the principles of complex variables and boundary elements. Heterogeneity is described by a large number of non-overlapping homogenous inclusions with mutually differing conductivities, which are embedded into the homogeneous background medium (multi-indicator structure). This procedure is perfectly suited for parallel processing, because the final solution can be obtained as a superposition of all particular solutions for each inclusion. The drawback of the AEM is that it is only valid for systems with multi-indicator heterogeneity structure.

Multi-scale adaptive methods based on wavelets and/or splines deserve special attention (e.g., Ebrahimi and Sahimi, 2002; Vasilyev and Kevlahan, 2005). These methods use the wavelet or spline basis functions only for the adaptive part of the solution, but the differential flow equation is solved by finite difference scheme on an adaptive non-uniform grid. There are also a few other promising approaches, such as the adaptive FE (e.g. Cao and Kitanidis, 1999) or spectral methods (Dykaar and Kitanidis, 1992; Van Lent and Kitanidis, 1996); however, these algorithms

suffer from the same serious disadvantages as all other aforementioned approaches.

The transport problem can be solved in an Eulerian approach, in terms of the advection-dispersion-reaction equation

$$\frac{\partial c}{\partial t} + \mathbf{v} \cdot \nabla c = \nabla \cdot (\mathbf{D} \cdot \nabla c) + S(c) \qquad (4)$$

where c is a concentration (M/L^3), $\mathbf{v}=\mathbf{q}/n$ is a velocity (L/T) obtained from Darcy's Law (Eq. 1), n (-) is a porosity, $\mathbf{D}$ (L^2/T) is a dispersion tensor and S (M/L^3T) is a reaction term (Helmig, 1998). All aforementioned approaches can be implemented for solving the transport problem (except AEM). However, for advection dominated problems with high Peclet number (ratio between advective and dispersive flux), significant numerical dispersion and/or oscillations occur, especially for more complex flow regimes such as the density driven flow examples (e.g. Voss and Souza, 1987; Gotovac et al., 2003). Therefore, the common practice is to use Lagrangian methods, such as particle tracking, which only require knowledge of the velocity field to obtain the ODE solution, according to the following system of equations (e.g. Hassan et al, 1998; Salandin and Fiorotto, 1998)

$$\frac{d X_i}{d t} = v_i(x, y) \;; \quad i = x, y \qquad (5)$$

where $\mathbf{X}$ is a position vector (L), which can easily be transformed into concentration or solute flux (M/L^2T). Particle tracking describes only advective transport, and presents a sub-model of more general random walk methods, which incorporate the influence of pore-scale dispersion into system (5) (Kinzelbach, 1988; LeBolle et al., 1996). These methods are attractive as they eliminate the influence of numerical dispersion, but cannot always describe general initial and boundary conditions.

1.2.2 Stochastic methods

Geostatistical methods have usually been employed to characterize the heterogeneity as an SRF (Kitanidis, 1997; Deutsch and Journel, 1998; Christakos, 2000). The spatial distribution is represented by the covariance (in the case of finite variance), or more generally by a variogram. A multi-Gaussian heterogeneity field is commonly assumed. This field is completely characterized by the first two statistical moments, and zones of low and high conductivity are practically uncorrelated. However, one of the most important features of flow and solute transport in heterogeneous porous media is a correlation of low and high conductivity zones, which can be described by indicator kriging (e.g. Gomez-Hernandez and Wen, 1998). The degree of heterogeneity is closely related to the selection of the variance of the log-conductivity. Roughly speaking, heterogeneity is defined to be low if the variance is less than one, mild for variances up to three, and high for variances greater than three. Gelhar (1993) reported many field experiments, some of which exhibited high heterogeneity, while Zinn and Harvey (2003) summarized field reports with variances as large as 10 or even 20. This means that both large and small variability's in the log-conductivity have been found in nature.

Generally, flow and transport in porous media have been analyzed mostly by analytic perturbations (Green's function method; e.g. Dagan, 1989; Rubin 1990; Neuman and Zhang, 1990; or spectral techniques; e.g. Bakr et al., 1978; Gelhar and Axness, 1983; Gelhar, 1993) or Monte-Carlo (MC) methods (using one single realization and ergodicity; Ababou et al., 1989; Thompson and Gelhar, 1990; Janković et al., 2003; or many MC realizations and ensemble averaging; Bellin et al., 1992, Cvetković et al., 1996, Salandin and Fiorotto, 1998, Hassan et al., 1998; de Dreuzy et al., 2007).

The main result of a flow analysis is velocity statistics. Among others, Rubin (1990) and Rubin and Dagan (1992) obtained velocity covariances for 2-D and 3-D isotropic and anisotropic porous media, using first-order analytic perturbation methods. More complicated second-order flow results were obtained by Dagan (1994), Deng and Cushman (1995), Hsu et al. (1996) and Hsu and Lamb (2000). Generally, second-order corrections only produce changes in the velocity variance. Salandin and Fiorotto (1998) numerically proved the results of first- and second-

order theory for cases of low and mild heterogeneity. Transport analysis will be presented in the next subsection.

Analytic perturbation methods are usually limited by several assumptions (Rubin, 2003): 1) small variance of the log-conductivity, 2) infinite domain, 3) steady–state flow, 4) uniform-in-the-average flow, 5) calculation of only the first two moments and 6) multi-Gaussian heterogeneity structure. While this thesis is focused on flow and transport in highly heterogeneous porous media, characterized by high lnK variance, the first assumption is the main constraint of the analytic methods in the present analysis. On the other hand, the Monte-Carlo method is the most general stochastic concept (without the above assumptions) for analyzing flow and transport in porous media, and is capable of producing the complete probability density function (pdf) and all necessary higher-order moments of the desired SRF variables. Analytic methods are mainly focused on evaluation of only the first two moments, assuming a Gaussian pdf for the SRF variables.

The Monte-Carlo method, in the Eulerian-Langragian formulation, consists of the following steps: 1) generation of as many log-conductivity realizations as possible, with predefined correlation structure, 2) numerical approximation of the log-conductivity field, 3) numerical solution of the flow equation with prescribed boundary conditions, in order to produce head and velocity approximations, 4) evaluation of the displacement position of a large number of the particles, 5) repetition of steps 2-4 for all realizations and 6) statistical evaluation of flow and transport variables such as head, velocity, travel time, transverse displacement, solute flux or concentration (including their cross-moments). Note that all previously mentioned numerical methods can be used for deterministic solutions of flow and transport in each realization. Therefore, the MC method lies between stochastic and numerical methods, because each step is solved numerically, but the overall solution is completely stochastic.

Although the MC method is appealing in its conceptual simplicity and generality, its benefits should be weighed against the large computational effort it requires for several reasons: large domains, huge linear or nonlinear systems of equations, a significant number of particles and realizations or extensive memory storage and CPU time requirements. Furthermore, each above mentioned step potentially presents a serious source of errors, especially for highly heterogeneous aquifers. The first step was successfully solved by construction of accurate conductivity random field generators (Bellin and Rubin, 1996, Deutsch and Journel, 1998). All other steps include numerical errors due to properties of the chosen method, discretization level, different types of averaging, upscaling and non-adaptive numerical modeling (without control of the local and global error). Particularly, key errors lie in step 3, as very fine spatial scales are required to solve detailed properties of the highly heterogeneous conductivity field described by the differential flow equation. In step 4, errors can arise due to an insufficient number of particles and inappropriate numerical integration of the trajectories and in step 6, an insufficient number of MC realizations prevents minimization of the statistical error of the higher moments and pdfs (Rubin, 2003).

A generally accepted conclusion confirms very good agreement between perturbation theory and MC for log-variances less than unity. Acceptable agreement was also shown for mild heterogeneity (log-variance up to 2), but there is no strong evidence for agreement between analytic and MC simulations in highly heterogeneous porous media (log-variance equal or greater than 4).

Some important moment equation methods have been obtained by techniques that expand equations (3-5) in terms of the first few statistical moments of the flow (e.g. Di Frederico and Neuman, 1998; Zhang and Li, 2004); this also applies to the transport analysis (e.g. Graham and McLaughlin, 1989a, b; Andričević, 1998, 2008). The main problem is choosing the assumptions needed for closure of the flow and transport problems. Usually, the assumptions employed limit the applicability of these results.

Recently, a few novel stochastic concepts have been developed to try to attain the

performance of the MC method in a more computationally efficient way. The first is the BME approach (Christakos, 2000) based on **B**ayesian conditioning and the **M**aximum **E**ntropy principle (Shannon, 1948; Jaynes, 1957). This approach is divided into three steps: i) the prior stage, which generates a prior pdf based on epistemic or general knowledge (variograms, differential equations, empirical relationships and so on), ii) the metaprior stage, which site-specific knowledge in an appropriate stochastic form and iii) the posterior stage which incorporates the general (i) and the site-specific knowledge (ii) into the form of the final posterior pdf at each space/time point. The BME approach, among others, has been presented for flow (Serre et al., 2003) and transport analysis (Kolovos et al., 2002). The BME approach is theoretically and practically sound, because it easily represents both hard and soft data, while the stochastic output is as general as in the MC case.

The second important technique is illustrated by the probability collocation method (PCM; Li and Zhang, 2007; Lin and Tartakovsky, 2009; Shi et al., 2009), which is directly related to the MC method. The PCM expands the log-conductivity in a Karhunen-Loeve (KL) expansion, and a deterministic problem is solved for each set of collocation points, rather than for sample points/elements in each spatial realization, as in a standard MC standard. Therefore, the number of simulations can be significantly reduced for flow and transport problems, while the accuracy of the MC method is maintained. Moreover, the computational efficiencies of both of these novel stochastic methods, i.e. BME and PCM, are significantly decreased in the presence of high heterogeneity, small correlation length (larger domain) or non-Gaussian structures, when the number of unknown coefficients increases the dimensionality of the problem to larger than 50 (Lin and Tartakovsky, 2009).

1.3 Solute transport concepts

Since flow in heterogeneous porous media is conceptually well-defined (e.g. Zhang, 2002), solute transport has been formulated in many ways. Solute transport analysis presents two basic dilemmas: Eulerian vs. Lagrangian frameworks, and resident concentration vs. solute flux approaches. While the Eulerian framework is closely related to the resident concentration via the advection-dispersion-reaction equation (4), the Langrangian framework is a more elegant and flexible, and is capable of solve both aforementioned approaches. Generally, there are a lot of important topics in both frameworks, such as advective transport (e.g. Salandin and Fiorotto, 1998; Janković et al., 2003), concentration fluctuations (e.g. Graham and McLaughlin, 1989; Kapoor and Gelhar, 1994; Kitanidis, 1994; Andričević, 2008), the influence of pore-scale dispersion (e.g. Kitanidis, 1994; Dagan and Fiori, 1997; Andričević, 1998; Fiori and Dagan, 1999, 2000), reactive transport (e.g. Cvetković and Dagan, 1994a, 1994b; Cvetković et al., 1998) and risk assessment (e.g. Andričević and Cvetković, 1996; Maxwell et al., 1999).

However, most Langrangian transport studies have been focused on macrodispersion (the second derivative of the displacement vector **X**), using analytic (e.g. Gelhar and Axness, 1983; Dagan, 1984, 1985, 1987, 1989; Rubin, 1990; Hsu et al., 1996; Hsu, 2003) or numerical methods (e.g. Bellin et al., 1992; Salandin and Fiorotto, 1998; Janković et al., 2003, Fiori et al., 2006, de Dreuzy et al., 2007).

This thesis focuses on travel time statistics, which is the heart of the solute flux approach, and analysis of three basic Langrangian transport variables, such as transverse displacement, travel time and Langrangian velocity. The general concept of the solute flux approach is given in the works of Dagan et al. (1992) and Cvetković et al. (1992). Travel time statistics are discussed analytically in Cvetković and Dagan (1994), Destouni and Graham (1995), Andričević and Cvetković (1998) and Fiori et al. (2002). Numerically, particle tracking methods were used to derive the travel time statistics, as reported in Bellin et al. (1992, 1994), Selroos and Cvetković (1992), Selroos (1995), Cvetković et al. (1996), Maxwell et al. (1999) and Hassan et al. (2001).

The classic description of breakthrough curves through the control plane can be obtained using the classic advection dispersion equation (ADE, Kreft and Zuber, 1978). Transport is Fickian and Gaussian if the mass distribution through the control plane satisfies ADE with a finite and constant longitudinal dispersion coefficient. It is worth mentioning that different conceptual strategies have been developed for non-Fickian or anomalous transport, such as the fractional diffusion equation (Benson et al., 2000), nonlocal transport approaches (Cushman and Ginn, 1993; Neuman and Orr, 1993), Boltzman transport equation (Benke and Painter, 2003) and continuous random walk methods (Scher et al., 2002, Berkowitz et al., 2002).

1.4 Motivation and objective of the research

Because of the obvious limitations and difficulties of carrying out physical experiments on flow and solute transport in heterogeneous porous media, computational methodologies have always been an indispensable part of theoretical and practical advances. Comparison of the advantages and disadvantages of all aforementioned methods show that our interpretation cannot be perfect, and there is no existing method that satisfies all of the requirements.

Nevertheless, the careful analysis of the last few subsections presents the state of the art of flow and transport subsurface modeling, and possible "room" for improvements. The aim of the research in this thesis is twofold. The first goal is the development of a general, accurate and adaptive multi-resolution framework, based on atomic Fup basis functions that can be applied to many subsurface problems and is closely related to the understood physical interpretation of the system. The second aim is the application of the presented methodology to problems with sharp fronts and narrow transition zones, which are useful for reactive transport, density driven and multiphase flow problems, and implementation of the methodology to calculate flow and advective transport in highly heterogeneous porous media, considering the influence of higher moments on the ensemble statistics.

2 METHODS

2.1 Eulerian and Lagrangian approach

Flow and transport in heterogeneous porous media can be considered with the Eulerian or Lagrangian approach (Rubin, 2003). The Eulerian approach considers mass conservation in arbitrary control volumes, elements or points and naturally describes deterministic problems using classic numerical methods (flow equation (3) and/or transport equation (4); e.g., Helmig, 1998) or moment stochastic equations using the closure assumptions (e.g., Graham and McLaughlin, 1989a, b; Andričević, 2008). The main feature of the Eulerian approach is a consideration of all flow and transport variables in the global static coordinate system.

On the other hand, the Lagrangian approach considers particles and their displacements and/or travel times in a moving coordinate system that "travels" with them. This framework is ideal for advection-dominated problems where particles move only along streamlines, without any influence from classical numerical dispersion. Since pore-scale dispersion can be added as a random movement to the particles between streamlines (Fiori and Dagan, 2000) or reactions in the t-τ domain (Cvetković and Dagan, 1994a, b), the Lagrangian approach is used for transport analysis, while flow problem is considered with the Eulerian approach in order to obtain velocity statistics.

2.2 Solute flux conceptual framework

In this thesis, the solute flux conceptual framework will be used due to its generality and simplicity in transport analysis. This framework can replace the classical resident concentration framework (related to Eq. 4) and naturally supports the beauty of the Lagrangian approach, providing a strong relation with measurements and real-site applications (Shapiro and Cvetković, 1988; Dagan et al., 1992; Cvetković et al., 1992). Without loss of generality, 2-D transport is considered under mean uniform flow (Figure 1) in terms of solute flux q(y, t; x), defined as the mass of solute per unit time and unit area through a control plane (CP) perpendicular to the mean flow direction.

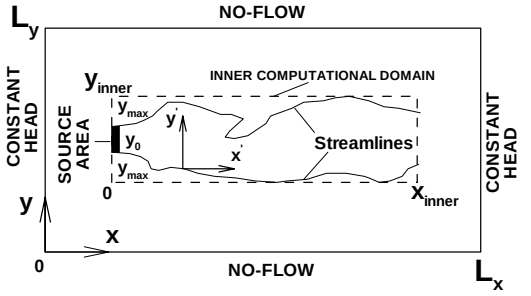

Figure 1. Simulation domain needed for global flow analysis and inner computational domain needed for flow and transport ensemble statistics.

Solute flux is regarded as a random variable of the transverse displacement y and travel time t for any control plane-x, due to random velocity field as a direct consequence of the natural uncertainty of hydraulic conductivity. The associated solute flux $\Delta q(y, t; x, a, t_0)$ for a particle with mass Δm injected at x=0 and y=a is defined as the rate of solute transfer through the CP (at x) at position y and time t

$$\Delta q(y,t;x,a,t_0) = \Delta m\, \delta(y-\eta)\, \delta(t-\tau) \quad (6)$$

where η is the transverse displacement in which the particle crosses the CP and τ is the travel time at which the particle crosses the CP. This means that the pdf of the solute flux is completely determined by the pdf of transverse displacement and travel time. For instance, the expected value of solute flux is defined as follows:

$$\langle \Delta q \rangle = \int_{t_0}^{\infty} \int_{-\infty}^{\infty} \Delta q\, d\eta\, d\tau = \Delta m\, g_1(y,t;x,a,t_0) \quad (7)$$

where solute flux is proportional to the joint pdf of transverse displacement and travel time (g_1). For advective transport, transverse displacement and travel time are independent. It will require general definitions for τ and η along streamlines using the total velocity in order to account for backward flow and multiple-crossings (paper III).

Let l denote the intrinsic coordinate (length) along a streamline/trajectory originating at y=a and x=0; I shall omit a in the following expressions for simplicity. The trajectory function can be parameterized using l as $[X_x(l), X_y(l)]$, and it can be written as

$$\tau(x) = \int_0^{l(x)} \frac{1}{v\left[X_x(\xi), X_y(\xi)\right]} d\xi \quad (8)$$

$$\eta(x) = \int_0^{l(x)} \frac{v_y\left[X_x(\xi), X_y(\xi)\right]}{v\left[X_x(\xi), X_y(\xi)\right]} d\xi \quad (9)$$

The transformation $\xi = (l(x)/x)\varsigma \equiv \lambda(x)\varsigma$ (where λ, which is always greater than one for a heterogeneous aquifer, is the dimensionless ratio of the length of the streamline and the distance x between the source line and the control plane) for any x>0 will give

$$\tau(x) = \int_0^x \frac{\lambda(x)}{v\left[X_x(\varsigma), X_y(\varsigma)\right]} d\varsigma \equiv \int_0^x \alpha(\varsigma; x) d\varsigma \quad (10)$$

$$\eta(x) = \int_0^x \frac{v_y\left[X_x(\varsigma), X_y(\varsigma)\right]}{v\left[X_x(\varsigma), X_y(\varsigma)\right]} \lambda(x) d\varsigma \equiv \int_0^x \beta(\zeta, x)\, d\zeta \quad (11)$$

where $w(\varsigma) \equiv v / \lambda$ is the Lagrangian velocity and $v_y(\varsigma)$ is its velocity transverse component. (I refer to $w(\varsigma)$ as the "Langrangian velocity".) In (10), α is referred to as the "slowness", while in (11), β is referred to as the streamline slope function, or simply "slope". It should be noted that in this approach, all Lagrangian quantities depend upon space rather than time, as in the traditional Lagrangian approach (e.g., Taylor, 1921; Dagan, 1984).

The first two moments of τ and η are computed as

$$\tau_A(x) \equiv E(\tau) = \int_0^x \alpha_A(\xi)\, d\xi$$

$$\sigma_\tau^2(x) \equiv E\left[(\tau - \tau_A)^2\right] = \int_0^x \int_0^x C_\alpha(\xi', \xi'')\, d\xi' d\xi''$$

$$\eta_A(x) \equiv E(\eta) = 0;$$

$$\sigma_\eta^2(x) \equiv E(\eta^2) = \int_0^x \int_0^x C_\beta(\xi', \xi'') d\xi' d\xi'' \quad (12)$$

Furthermore, higher moments of the travel time and transverse displacement are completely defined by the statistics of the slowness and slope. The travel time pdf and higher moments can be obtained more efficiently with the aid of the cumulative distribution function-CDF (Ezzedine and Rubin, 1996) of the travel time (the same for transverse displacement and other Lagrangian transport variables)

$$F_\tau(t; x) = \frac{1}{N_P n_{MC}} \sum_{i=0}^{N_P} \sum_{j=1}^{n_{MC}} (H(t - \tau(x))) \quad (13)$$

; (1)

where H is the Heaviside function, N_P is the number of particles, and n_{MC} is the number of Monte-Carlo realizations. Travel time in (13) has the form (10) for each particular particle and realization; therefore, expectation in (13) is made over all realizations and particles from the source. The probability density function is obtained simply as $f_\tau(t; x) = \partial(F_\tau(t; x))/\partial t$. The travel time mean is computed as $\tau_A(x) = \int_0^\infty t\, f_\tau(t; x)\, dt$.

Higher travel time moments (such as variance) are obtained directly from the pdf as

$$M_i^\tau(x) = \int_0^\infty (t - \tau_A(x))^i f_\tau(t; x)\, dt; i = 2,3,..., \infty.$$

2.3 Atomic basis functions

In this thesis, adaptive multi-resolution methodologies based on Fup basis functions are developed and presented. Since Fup basis functions belong to the family of atomic basis functions, the aim of this subsection is to provide a general presentation of these types of basis functions with compact support, which allow for the development of promising new methodologies in subsurface hydrology and related applied sciences. Therefore, this subsection describes Fup basis functions, but also gives an overview of other atomic basis functions.

2.3.1 Definition

Atomic basis functions are compactly supported and infinitely differentiable functions (Rvachev and Rvachev, 1971; Gotovac and Kozulić, 1999). Atomic functions are defined as solutions of differential-functional equations of the following type

$$L_D y(x) = \lambda_D \sum_{k=1}^{M} C_k\, y(ax - b_k) \quad (14)$$

where L_D is a linear differential operator with constant coefficients, λ_D is a non-zero scalar, C_k are coefficients of the linear combination, a>1 is a parameter defining the length of the

compact support and b_k are coefficients that determine the displacements of the basis functions. Different linear operators and related parameters define different types of atomic basis functions.

Rvachev and Rvachev (1971) in their pioneer work called these basis functions "atomic" because they span the vector spaces of all three fundamental functions in mathematics: algebraic, exponential and trigonometric polynomials. Additionally, atomic functions can be divided into an infinite number of small pieces that maintain all of their properties, implying a so-called "atomic structure".

2.3.2 Up(x) and Fup$_n$ (x) basis functions

The simplest function, which is the best studied among atomic basis functions, is the up(x) function. The up(x) function is a smooth function with compact support [-1,1] obtained as a solution of the differential-functional equation

$$up'(x) = 2\,up\,(2x+1) - 2\,up\,(2x-1) \qquad (15)$$

with the normalized condition $\int_{-\infty}^{\infty} up(x)dx = 1$, while Rvachev (1982) and Gotovac and Kozulić (1999) provided a tractable means for calculating the up(x) function instead of using its Fourier transform

$$up(x) = 1 - \sum_{k=1}^{\infty}(-1)^{1+p_1+\ldots+p_k}\,p_k \sum_{j=0}^{k} C_{jk}\,(x-0, p_1 \ldots p_k)^j \qquad (16)$$

where the coefficients C_{jk} are rational numbers determined according to the following expression

$$C_{jk} = \frac{1}{j!}\,2^{j(j+1)/2}\,up(-1+2^{-(k-j)}); \quad j = 0,1,\ldots,k; \quad k = 1,2,\ldots,\infty \qquad (17)$$

Calculation of $up(-1+2^{-r}); r \in [0,\infty]$ in the binary-rational or characteristic points of a dyadic grid and all of the details regarding the calculation of up(x) function values are provided in Gotovac and Kozulić (1999). The argument (x-0, p_1 ... p_k) in Eq. (16) is the difference between the real value of coordinate x and its binary form with k bits, where p_1 ... p_k are digits, 0 or 1, of the binary development of the coordinate x value. Therefore, the accuracy of the coordinate x computation, and thus the accuracy of the up(x) function at an arbitrary point, depend upon machine accuracy. From Eq. (15), it can be seen that the derivatives of the up(x) function can be calculated simply from the values of the function itself.

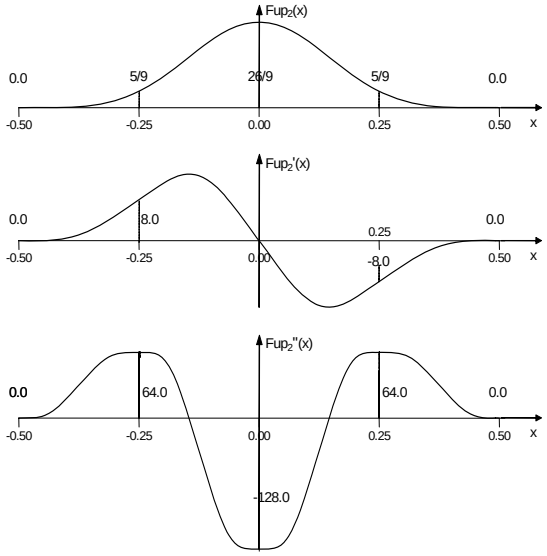

Figure 2. Function Fup$_2$(x) and its first two derivatives.

The Fup$_n$(x) function satisfies the following differential-functional equation

$$Fup'_n(x) = 2\sum_{k=0}^{n+2}\left(C_{n+1}^{k} - C_{n+1}^{k-1}\right) Fup_n(x)\left(2x - 2^{-n-1}k + 2^{-n-2}(n+2)\right) \qquad (18)$$

where n is the Fup order. For n=0, Fup$_n$(x)=up(x) since Fup$_n$(x) and its derivatives can be calculated using a linear combination of displaced up(x) functions instead of using their Fourier transforms

$$Fup_n(x) = \sum_{k=0}^{\infty} C_k^*(n)\,up\left(x - 1 - \frac{k}{2^n} + \frac{n+2}{2^{n+1}}\right) \qquad (19)$$

where $C_k^*(n)$ are auxiliary coefficients obtained from a suitable recursive formula (Gotovac and Kozulić, 1999). Fup$_n$(x) is defined on the compact support [-(n+2)2^{-n-1},

$(n+2)2^{-n-1}$]. Figure 2 shows the $Fup_2(x)$ function and its first two derivatives, which are primarily used in this thesis (papers I-V).

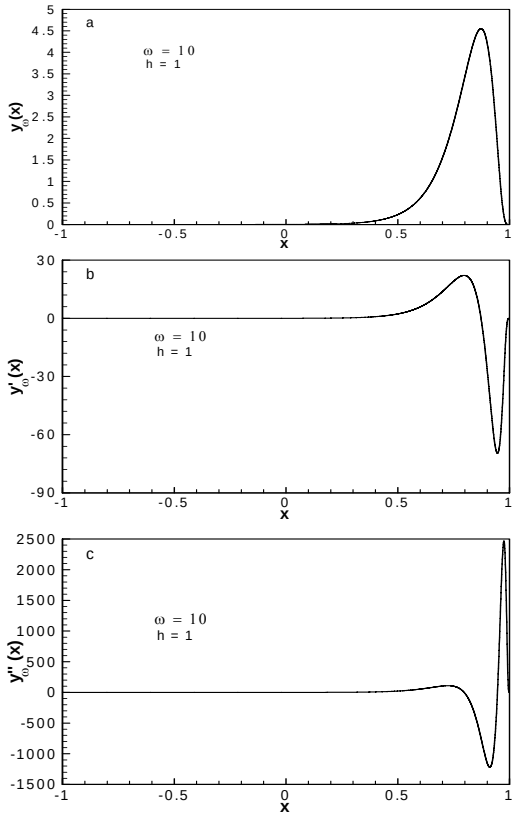

Figure 3. Function $y_{10}(x)$ and its first two derivatives.

Index n also denotes the highest degree of the algebraic polynomial which can be expressed exactly in the form of a linear combination of n+2 $Fup_n(x)$ basis functions displaced by a characteristic interval 2^{-n}. Thus, a quadratic polynomial on a characteristic interval 2^{-n} can be exactly presented as follows

$$x^2 = 2^{-6}\sum_{k=-1}^{2}\left(k^2 - 5/18\right)Fup_2\left(x - k/4\right) \qquad (20)$$

2.3.3 Exponential and trigonometric atomic basis functions

Exponential basis functions satisfy the following differential-functional equation

$$y'_\omega(x) - \omega\, y_\omega(x) = a_\omega y_\omega(2x+1) - b_\omega y_\omega(2x-1) \qquad (21)$$

where ω is a frequency defined on the compact support [-1, 1], $a_\omega = \dfrac{\omega\exp(-\omega/2)}{sh(\omega/2)}$ and $b_\omega = a_\omega\exp(\omega)$ are related parameters. Note that Eq. (21) can be generalized for any h. They can be calculated using their Fourier transform

$$y^*_\omega(s) = \prod_{j=1}^{\infty}\frac{\omega}{2\,sh(\omega/2)}\frac{sh(\omega/2 + j\,s\,2^{-j})}{\omega/2 + j\,s\,2^{-j}} \qquad (22)$$

An exponential basis function with its first two derivatives and ω=10 is presented in Figure 3.

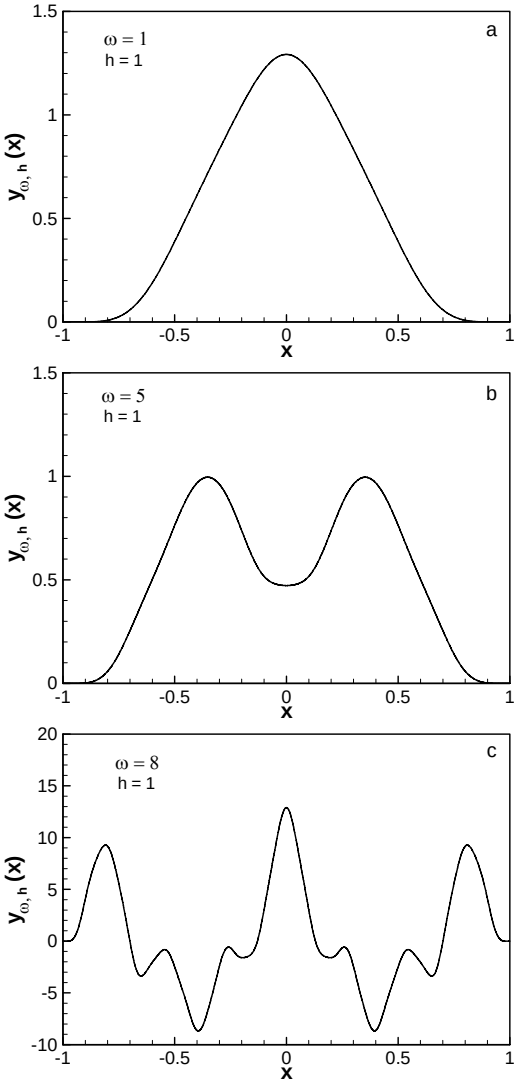

Figure 4. Function $y_{\omega,h}(x)$ with h=1 and a) ω=1, b) ω=5 and c) ω=8.

Trigonometric basis functions satisfy the following differential-functional equation

$$y''_{\omega,h}(x) + \omega^2\, y_{\omega,h}(x) = a_{\omega,h}y_{\omega,h}(3x+2h) - b_{\omega,h}y_{\omega,h}(3x) + a_{\omega,h}y_{\omega,h}(3x-2h) \qquad (23)$$

defined on the compact support [-h, h]. Parameters $a_{\omega,h} = \frac{3}{2}\frac{\omega^2}{1-\cos(2\omega h/3)}$ and $b_{\omega,h} = 2a_{\omega,h}\cos(2\omega h/3)$ completely define Eq. (23). They can be calculated using their Fourier transform

$$y^*_{\omega,h}(s) = \frac{2a_{\omega,h}}{3} \prod_{j=1}^{\infty} \frac{\cos(2sh/3) - \cos(2\omega h/3)}{\omega^2 - s^2/9^{j-1}} \quad (24)$$

Trigonometric basis functions with h=1 and ω=1, 5 and 10 are presented in Figure 4. Exponential and trigonometric atomic basis functions are defined by frequency and are directly related to the spectral Fourier analysis. They exactly describe exponential and trigonometric polynomials with frequency ω on the compact support [-h, h] with a linear combination of displaced basis functions. The original idea, which came from the application of atomic basis functions, is that the type of the basis function is chosen depending upon the problem and vector space that spans its exact solution (Gotovac, 1986).

2.3.4 Multi-dimensional radial atomic basis functions

Generalization of the atomic basis functions with compact support to many dimensions leads to the following type of functional-differential equations (Kolodyazhny and Rvachev, 2007)

$$L_D\, y(x) = \sum_{k=1}^{N} \int_{\partial\Omega_k} H_k(x)\, y(a\,x - \xi_k) + \sum_{l=1}^{M} y(a\,x - \alpha_l) \quad (25)$$

where $\partial\Omega$ is a closed contour (i.e., the boundary of a general convex domain). Kolodyazhny and Rvachev (2007) particularly generalized two- and three-dimensional basis functions for Laplace and bi-harmonic linear operators. These multi-dimensional basis functions are closely related to other radial basis functions (e.g., Kansa, 1990). Finally, they also presented a complete overview of atomic basis functions.

2.4 Adaptive Fup methodology

Subsurface processes are usually very complex and can be divided into many different types of flow and transport, such as density-driven and multiphase flow or non-reactive and reactive transport. Therefore, there is no universal methodology which describes all subsurface processes. In this thesis, an adaptive Fup multi-resolution methodology suitable for many groundwater flow and transport problems is developed and will be briefly presented in the sequel. A detailed description is given in the Appendix (related papers I-V).

2.4.1 Fup transformations

Fup transformations are versatile tools for the description of heterogeneity, pumping or recharge, as well as all other flow and transport variables that consist of different spatial and/or temporal scales. First, I present here the **F**up **C**ollocation **T**ransform (FCT), which is an efficient numerical tool for describing various types of data, signals and functions using a linear combination of the Fup basis functions (paper I). The main feature of the FCT is that specific frequencies and corresponding Fup coefficients are associated with a particular resolution level and spatial location, which is not possible in the classic discrete Fourier transform. The zero level is the starting (coarsest) level, which is always present in the grid. The FCT satisfies function values at all collocation points and related derivatives at boundary collocation points. The key step in the FCT is the transfer from the current level to the next level. The residual between the true function and the previous level approximation is checked and the points with a residual below the prescribed threshold are dropped from the grid. This procedure presents an a-priori adaptive criterion for defining the new collocation points at the next level. For the first and each subsequent level, the collocation algorithm should only satisfy the residual between the true function and its approximation from the previous levels. In other words, all Fup coefficients from previous levels are "frozen" and only Fup coefficients at the current level should be found. Higher levels include only higher frequencies and provide a

more detailed description of the chosen function.

The multi-resolution 2-D FCT of the function u(x,y) can be presented as

$$u^J(x,y) = \sum_{j=0}^{J} \sum_{k,l \in Z^j} d_{k,l}^j \varphi_{k,l}^j(x,y) \tag{26}$$

where J is an arbitrary chosen maximum level, Z^j is the irregular grid at each level, which contains only the significant collocation points and Fup basis functions needed for the Fup presentation in Eq. (26) with the desired accuracy defined by the threshold ε, $d_{k,l}^j$ are Fup coefficients, $\varphi_{k,l}^j$ are Fup basis functions and k and l represent the indexes of collocation points at the current level for the x and y directions, respectively. The zero level is defined by a chosen resolution level j_{minx} for the x-direction and by j_{miny} for the y-direction. Generally, a sparse linear system of equations can be obtained at each level j

$$\sum_{k,l \in Z^j} d_{k,l}^j \varphi_{k,l}^j(x_p^j, y_q^j) = \Delta_j(x_p^j, y_q^j) \quad , \tag{27}$$
$$p,q \in Z^j : 0 \le p \le 2^{j_{\min x}+j} \, , \, 0 \le q \le 2^{j_{\min y}+j}$$

$$\sum_{k,l \in Z^j} d_{k,l}^j \varphi_{k,l}^{j\,(m_x,m_y)}(x_p^j, y_q^j) = \Delta_j^{(m_x,m_y)}(x_p^j, y_q^j),$$
$$p,q \in Z^j : (p = 0 \ or \ p = 2^{j_{\min x}+j} \tag{28}$$
$$or \ q = 0 \ or \ q = 2^{j_{\min y}+j})$$
$$and \quad (m_x > 0 \ or \ m_y > 0)$$

where m_x and m_y are the orders of the derivative in the x and y directions, respectively. System (27-28) presents conditions for satisfying function values within the domain (27) and partial derivatives at the boundary points (28). The residual vector on the right side presents the residual between the real function and its approximation, including all previous levels.

The main drawback of the FCT is the solving of the sparse linear system of equations at each level (27-28). The **F**up **R**egularized **T**ransform (FRT) has the same purpose and uses the exact same adaptive strategy as the FCT, but directly connects function or data values with Fup coefficients (without solving the system 27-28), using at each collocation point the local equivalence between the Fup and a polynomial approximation (paper II). Therefore, FRT exactly describes polynomials up to the Fup order. FCT requires a slightly less number of collocation points than FRT for a general function.

The two Fup transformations used in this thesis are only two selected choices, and many other transformations are possible to create by utilizing different conditions for system (27-28). For instance, two more important transformations can be very appealing in practice: i) the Fup Galerkin Transformation, which uses Fup basis functions as test functions, and ii) the Maximum Entropy Fup Transformation, in which system (27-28) is replaced with a nonlinear system of Fup moment equations utilizing the maximum entropy principle (related to paper V).

2.4.2 Adaptive Fup Collocation Method

Kozulić and Gotovac (2000) and Gotovac et al. (2003) developed non-adaptive collocation solutions for boundary-value problems in structural mechanics and density-driven flow, respectively. Moreover, initial value problems have been presented by Gotovac and Kozulić (2002). This thesis develops two suitable forms of the **A**daptive **F**up **C**ollocation **M**ethod (AFCM).

First, AFCM that are well suited for spatial-temporal solutions with sharp fronts were developed through the method of lines (paper I). An AFCM consists of three commonly used basic steps (Figure 5; e.g., Vasilyev and Bowman, 2000; Cruz et al., 2003)

a) Spatial grid adaptation,
b) Calculation of spatial derivatives,
c) Time integration.

The spatial adaptive procedure is performed after each time step according to the presented FCT and the corresponding adaptive strategy. This procedure dynamically changes the grid and significantly reduces computational cost. A solution from the initial conditions or previous time step is described by FCT. All FCT points are called basic points since they create the basic grid. Apart from basic points (which are related to the FCT a-priori adaptive criterion), additional points

are needed for consistent approximation of the system dynamics (temporal solution changes) during the calculated adaptive time step, Δt. Basic and additional points create the total grid needed for the description of the system dynamics from time T to time $T+\Delta t$. The basic hypothesis behind the algorithm (during the time step Δt) is that the solution does not "move" outside the border of the adapted non–uniform grid. Finally, the total grid needs to be transformed into an effective grid suitable for time integration.

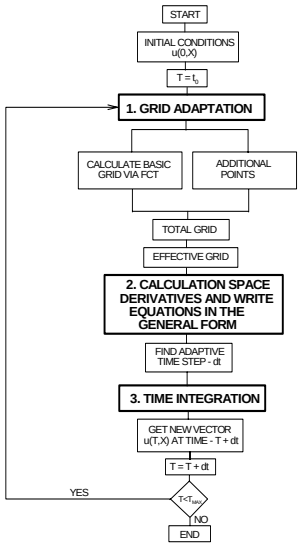

Figure 5. Flow chart of the AFCM (paper I).

Time integration is obtained by solving a system of differential-algebraic equations, written in a general form suitable for groundwater flow and transport problems (in each time step):

$$A(t,u)\frac{\partial u}{\partial t} = F\left(t,x,u,u^{(m)}\right) \tag{29}$$

$$0 = G\left(t,x,u,u^{(m)}\right) \tag{30}$$

where u is the solution, m is the order of derivatives and A, F and G are linear or non-linear operators, depending upon the considered problem. The spatial derivatives in operators F and G must be written in a form that contains only function values closely related to the well-known finite-difference stencils. Equation (29) represents time–dependent partial differential equations which describe the time evolution of the solution, while the algebraic equations (30) present the boundary conditions (Dirichlet, Neumann or Chauchy mixed type).

The second application of the AFCM (papers II-III) solves the flow problem (3) with only Fup basis functions at each level using the collocation framework and an adaptive strategy similar to the FCT in the following way

$$\sum_{k,l\in Z^j} d_{k,l}^j \left(\frac{\partial^2 \varphi_{k,l}^j\left(x_p^j, y_q^j\right)}{\partial x^2} + \frac{\partial^2 \varphi_{k,l}^j\left(x_p^j, y_q^j\right)}{\partial y^2} \right) +$$
$$\frac{\partial Y\left(x_p^j, y_q^j\right)}{\partial x} \left(\sum_{k,l\in Z^j} d_{k,l}^j \frac{\partial \varphi_{k,l}^j\left(x_p^j, y_q^j\right)}{\partial x} \right) +$$
$$\frac{\partial Y\left(x_p^j, y_q^j\right)}{\partial y} \left(\sum_{k,l\in Z^j} d_{k,l}^j \frac{\partial \varphi_{k,l}^j\left(x_p^j, y_q^j\right)}{\partial y} \right) = \tag{31}$$
$$\Delta_j\left(x_p^j, y_q^j\right): 0 \le p \le 2^{j_{\min x}+j},$$
$$0 \le q \le 2^{j_{\min y}+j}, p,q \in Z^j$$

with boundary conditions:

$$\sum_{k,l\in Z^j} d_{k,l}^j \varphi_{k,l}^j(x_p^j, y_q^j) = \Delta_j^{(n_x,n_y)}(x_p^j, y_q^j) : \tag{32}$$
$$(p = 0 \ or \ p = 2^{j_{\min x}+j}, p,q \in Z^j)$$

$$\sum_{k,l\in Z^j} d_{k,l}^j \frac{\partial \varphi_{k,l}^j(x_p^j, y_q^j)}{\partial y} = \Delta_j^{(n_x,n_y)}(x_p^j, y_q^j) : \tag{33}$$
$$(q = 0 \ or \ q = 2^{j_{\min y}+j}, p,q \in Z^j)$$

for a given FRT approximation of the log-conductivity field Y. Each non-zero level solves only the residual of the flow equation and corresponding boundary conditions from all previous levels ("frozen" Fup coefficients) and gives particular head corrections (Fup coefficients at the current level). The adaptive criterion adds new collocation points in the next level only in the zones where the head correction is greater than the prescribed threshold.

2.4.3 Adaptive Fup Monte-Carlo Method

The **A**daptive **F**up **M**onte **C**arlo **M**ethod (AFMCM, paper II) follows the Eulerian-Lagrangian formulation, separates the flow from the transport problem and consists of the following common steps (see subsection 1.2.2; Rubin, 2003).

Figure 6 shows the flow chart of the AFMCM, which represents a general frame-

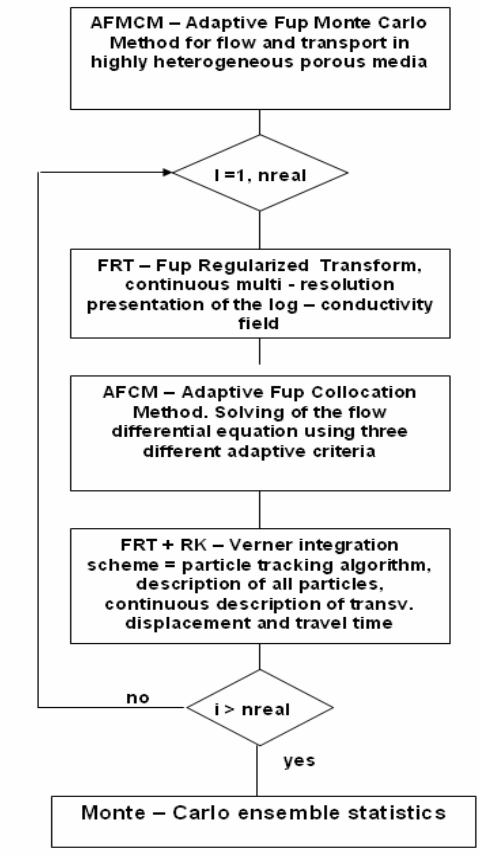

Figure 6. Flow chart of the AFMCM (paper II).

work for flow and transport in heterogeneous porous media (paper II).

AFMCM uses the random field generator HYDRO_GEN (Bellin and Rubin, 1996) for step 1 due to its accuracy and generality. Log-conductivity approximation (step 2) is solved by FRT, reproducing very accurately prescribed ensemble statistics. Step 3 uses an AFCM for the differential flow equation (3) in order to get an accurate and continuous velocity field in each realization. The positions of particles and related travel times are calculated with a new particle-tracking strategy (step 4) using the high-order Runge-Kutta-Verner (8-5:6) time integration scheme (Verner, 1978) and FRT. In that way, travel time and transverse displacement fields are described as continuous functions with prescribed accuracy. Finally, it is possible to extract an unlimited or desired number of particles from these solutions in order to eliminate statistical fluctuations in ensemble statistics. Ensemble statistics are described in a multi-resolution way (26) as all other mentioned fields in each realization (step 6; Figure 6). All mentioned MC methodology steps are detailed in paper II.

2.4.4 Inexact Fup Maximum Entropy algorithm

The maximum entropy (MaxEnt) principle is a versatile tool for statistical inference of the pdf from its moments as the least biased estimation among all other possible distributions. It maximizes Shannon entropy, subjected to the moment constraints (Shannon, 1948; Jaynes, 1957)

$$\max S(x) = -\int_{x_{\min}}^{x_{\max}} \ln(f(x))\, f(x)\, dx \tag{34}$$

$$\int_{x_{\min}}^{x_{\max}} h_i(x)\, f(x)\, dx = \mu_i \; ; i = 0,\ldots,m \tag{35}$$

where μ_i are moments of an arbitrary set of basis functions ($h_i(x)$; i=0,…,m), while f is an unknown pdf. The MaxEnt algorithm transforms the original constrained optimization problem to the unconstrained convex dual optimization problem using the Lagrangian multipliers. The classic moment problem uses algebraic power moments as basis functions and yields the pdf in the following form of Lagrangian multiplications

$$f(x) = \exp\left(-1 - \lambda_0 - \sum_{j=1}^{m} \lambda_j x^j\right) \tag{36}$$

This procedure is characterized by strong nonlinear system (combining Eq. 35 and system 36), which causes typical conventional numerical methods to fail for higher-order moments (m>5-10) due to different sensitivities of the Lagrangian multipliers and their unbalanced nonlinearities (Mead and Papanicolaou, 1984).

Classic MaxEnt algorithms overcome these difficulties by using orthogonal polynomials that enable roughly the same sensitivity as all Lagrangian multipliers (Turek, 1988; Bandyopadhyay et al., 2005; Abramov, 2007, 2009). Paper V presented a principally different idea, using the low order Fup_2 basis func-

tions with compact support which exactly describe algebraic polynomials up to the second order, but approximately describe other polynomials of higher order. Now, the related nonlinear system becomes numerically very efficient due to localized properties of the Fup basis functions, but consequently these basis functions approximately describe all moments of polynomials with order higher than the Fup order. Therefore, this algorithm is called the Inexact Fup Maximum Entropy Algorithm (IFMEA).

This algorithm is based on the following relation

$$x^i = \sum_{j=0}^{m} d_{ij} Fup_{2j}(x) + \varepsilon_i(x); i = 0,.,m \qquad (37)$$

where $\varepsilon_i(x)$ are residual functions that represent differences between monomials and their Fup_2 approximations. Furthermore, the relationship between their moments represents the iterative scheme of IFMEA

$$\mu_i - \Delta\mu_i^{(l-1)} = \sum_{j=0}^{m} d_{ij} \mu_j^{Fup_2(l)} \qquad (38)$$

where i=0,…,m is a moment index, l=1,2,…,∞ is an iteration step, while $\mu_i, \Delta\mu_i^{(l-1)}, \mu_j^{Fup_2(l)}$ are moments of monomials, residual functions and Fup_2 basis functions, respectively. Since the moments of residual functions and Fup_2 basis functions are unknown, the algorithm assumes residual moments from the initial pdf guess (l=0) or previous step (l>0). Then, the moments of the Fup_2 basis functions are calculated from the system (38). Thus, the classic moment problem is now reduced to the maximum entropy problem over the Fup_2 moments, which yields an approximation of the exact MaxEnt pdf (36)

$$f^*(x) = \exp(-1 - \sum_{j=0}^{m} \gamma_j Fup_{2j}(x)) \qquad (39)$$

The iterative algorithm is repeated until the convergence of respected Fup_2 moments. The final moment error is presented by

$$\mu_i - \mu_i^* = \int_{x_{\min}}^{x_{\max}} \varepsilon_i(x)(f(x) - f^*(x))\,dx \qquad (40)$$

Since the two integral functions are small relative to the monomials and the exact pdf, respectively, and they fluctuate around zero or very close to zero, the actual moment error is negligible for all practical papers (paper V).

3 RESULTS

3.1 Introduction

This Section represents the main thesis results and application of adaptive Fup multiresolution methodology in the short and straightforward way, while more detailed presentation is given in related papers I-V in Appendix.

3.2 Description of solutions with fronts and narrow transition zones (paper I)

Many groundwater flow and transport problems, especially those with sharp fronts, narrow transition zones, layers and fingers, require extensive computational resources. In paper I, AFCM based on *Fup* basis functions and method of lines (MOL) is presented. Procedure enables the adaptive multiresolution approach to solve problems with different spatial and temporal scales with a desired level of accuracy using the entire family of *Fup* basis functions.

Procedure can be presented on classic multiphase benchmark example - Buckley-Leveret problem. The problem is characterized by strong nonlinearities and a narrow saturation front. Moreover, the nonlinear system (29-30) is very stiff and requires short time steps. There is no analytic solution, but the problem has been solved numerically by Kurganov and Tadmor (2000) and Cruz et al. (2003) using a high resolution finite difference scheme.

Figure 7 shows a multilevel adaptive solution for the moving saturation front. Initial conditions are relatively simple except at one point where the saturation front has a discontinuous derivative. Therefore, five levels are needed for this simple bilinear function. At the early stages of the process the saturation front moves very slowly and at t = 0.1 reaches the final steepness and sharpness with eight levels and nearly 140 collocation points. After that, the front travels toward the right boundary, while adaptive grid follows its movement.

This example presents the efficiency of the method in handling strong nonlinear problems and the narrow saturation front with changes in sharpness and location, both in space and time. The adaptive grid follows the system dynamics and displays a wide range of different spatial and temporal scales that characterize this complex problem. The efficiency of the method is usually described by the compression coefficient (C_C) which is defined as a ratio between the number of collocation points in the non-adaptive and adaptive algorithm ($C_C = 2^{j_{\min}+j}/N_{AD}$). Namely, a non-adaptive algorithm would require all points at the maximum level in order to obtain the same accurate solution as the solution described by AFCM. The compression coefficient is about 30 which clearly show the efficiency of the proposed AFCM.

The method was also tested and verified (Figure 7) by comparison, at t = 0.2, between solutions obtained by AFCM and those by Cruz et al. (2003). Figure 7 shows an almost perfect match between the two solutions.

Final example is a 1-D density driven problem. Initial conditions are very demanding and show that the domain is filled by fresh water with a hydrostatic distribution. The pulse concentration boundary condition on the left side consists of the salt water source which enters the domain during the first part of the simulation ($t^* = 0.15$). After that, the concentration is zero (fresh water). The concentration boundary condition on the right side is defined by no-dispersion flux boundary. Both boundary pressure conditions are constant Dirichlet boundary conditions. Solution dynamics is presented in Figure 8.

AFCM solution uses four different concentration thresholds in order to present convergence test to the unknown exact solution, while Zegeling et al. (1992) used 100 points which are adaptively located inside the domain (Figure 8). However, AFCM and their solution are not in the close agreement due to a significant difference in the backward front. Reasons are twofold: a) Zegeling et al. (1992) considers a fixed number of points (e.g. N = 100). After the injection time their algorithm redistributes points around two fronts and loose accuracy and more important

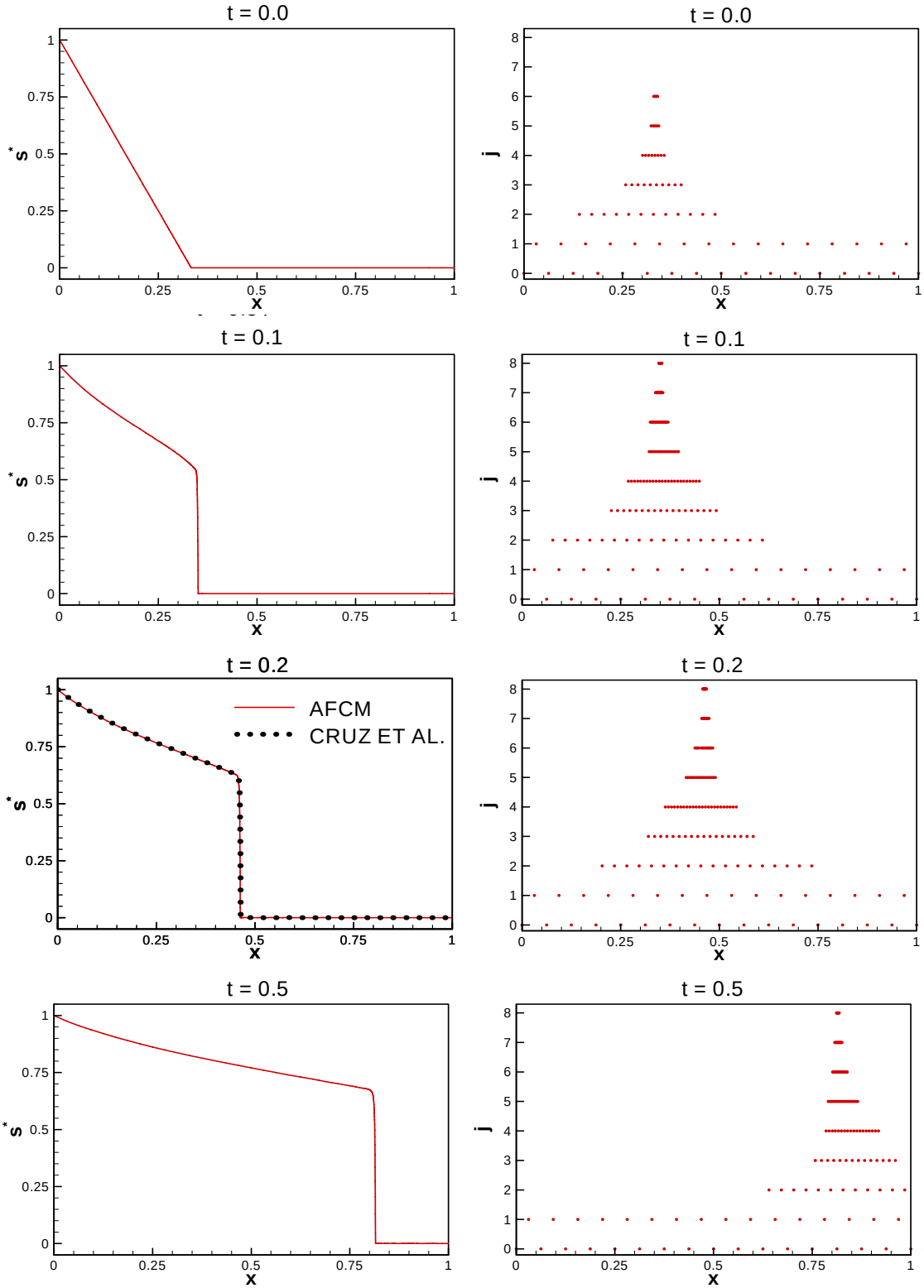

Figure 7. Saturation front (left) and adaptive grid (right) for the Buckley-Leverett problem at four selected time steps. Comparison between AFCM and Cruz et al. (2003) at t=0.2.

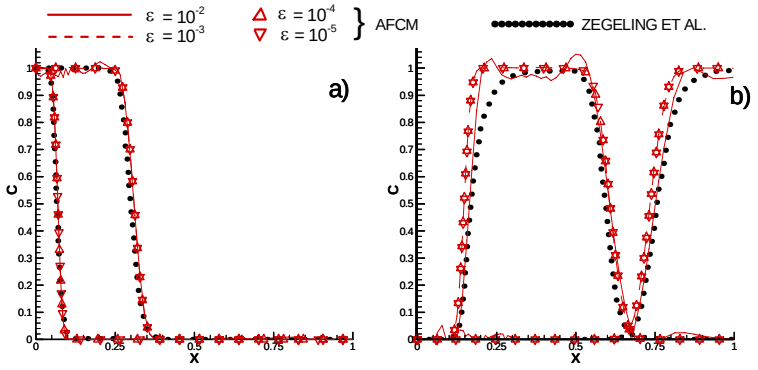

Figure 8. Comparison between AFCM and Zegeling et al. (1992) for 1-D vertical density driven flow and transport problem at a) t=0.02 and 0.1 and b) t*=0.2 and 0.4 with dispersion (α_L = 0.001 m) and the pulse concentration boundary condition at the left side.*

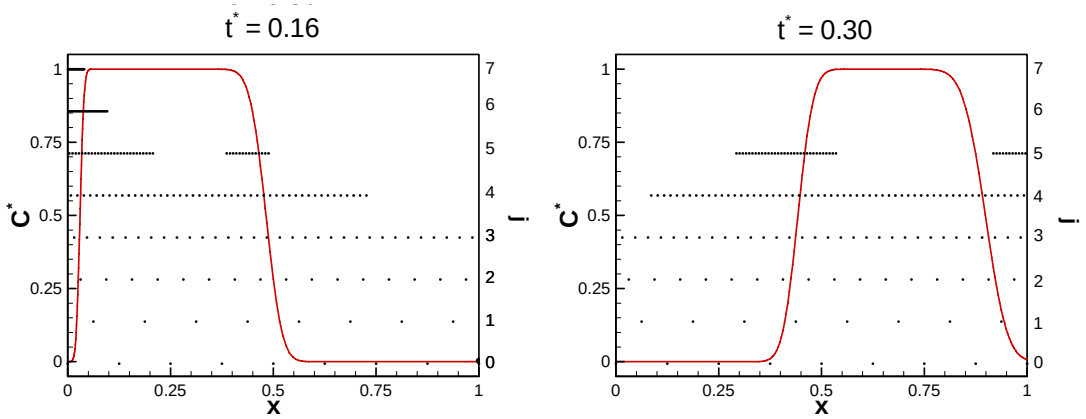

Figure 9. Concentration field and adaptive grid for 1-D vertical density driven flow and transport problem at t=0.16 and 0.30 with dispersion (α_L = 0.001 m), pulse concentration boundary condition on the left side and threshold* $\varepsilon_C = 10^{-4}$.

b) description of the shock concentration boundary condition at the start and end of the injection time due to creating very steep concentration front.

After the injection time, the backward front is steeper than the upward front due to the influence of the left concentration boundary condition. For threshold $\varepsilon_C = 10^{-4}$, at $t^* = 0.16$ Figure 9 shows that the grid follows two fronts while the backward front requires two additional resolution levels. After some time both fronts need the same resolution ($t^* = 0.30$).

During the simulation time the compression coefficient fluctuates between 20 and 40. Peclet number is a very high (Pe~20), since solution is stable and accurate (oscillations are 100 times less frequent than the prescribed threshold $\varepsilon_C = 10^{-4}$).

This procedure can be particularly attractive for reactive transport and other related problems with sharp fronts which exhibit a wide range of spatial and temporal scales.

3.3 Description of heterogeneity (paper II)

A single realization of the hydraulic conductivity obtained by HYDRO_GEN (Bellin and Rubin, 1996) is illustrated in Figure 10. A discrete set of generated log-conductivity values are transformed to the continuous function by the Fup collocation transform (FCT). FCT satisfies exactly generated grid values and elsewhere interpolation is closely related to the polynomial approximation of the n order if n is a Fup order (Fup_2 basis functions). Figure 10 shows a multi-resolution FCT approximation of the log-conductivity field in one chosen realization for $\sigma_Y^2 = 6$. HYDRO_GEN generates 32 grid values per integral scale with conductivity differences over seven orders of magnitude. Zero level satisfies minimum requirement of 2 collocation points per integral scale (n_Y=2).

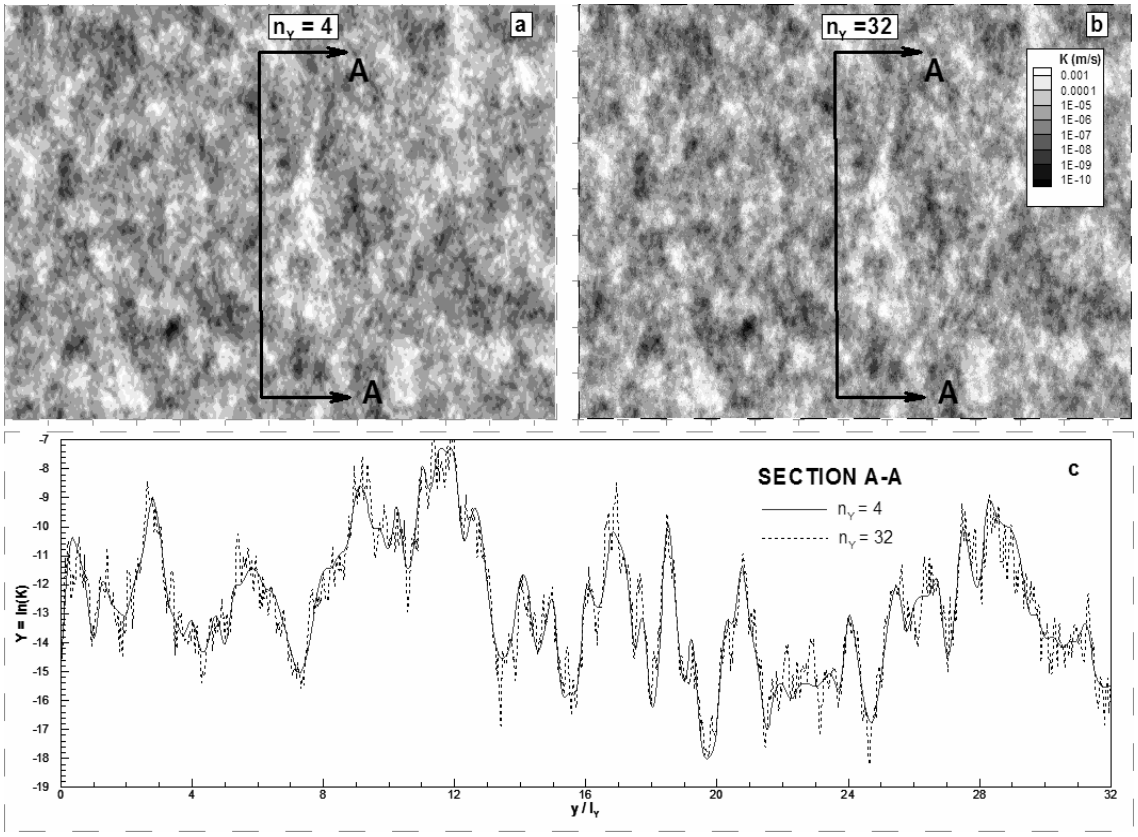

Figure 10. Multi-resolution Fup approximation of the (log)-conductivity field (one chosen multi-Gaussian realization) obtained by FCT with exponential covariance and σ_Y^2 =6 for different resolution levels (domain is 64I_Y *32I_Y): a) conductivity field for n_Y=4; j=1 , b) conductivity field for n_Y=32; j=4 which is also HYDRO_GEN resolution level and c) log-conductivity field for section A-A, n_Y=4 and n_Y=32.

First level is two times denser, 4 points per integral scale (n_Y=4, Fig. 10a), while second, third and fourth levels consist of n_Y=8, 16 and 32 (Fig. 10b) collocation points per integral scale, respectively. Final, fourth level exactly reproduces all HYDRO_GEN values, but interestingly visual inspection does not reveal any difference between the first and fourth levels. However, in cross section A-A (Fig. 10c) differences between different resolution levels exist only at higher level points.

Accuracy of the HYDRO_GEN and FCT is shown on Figure 11 for 500 MC realizations and $\sigma_Y^2 = 6$. Prescribed and reproduced correlations (Figure 11a) and distributions (Figure 11b) are identical due to collocation nature of the algorithm. On the other side, FRT slightly modifies HYDRO_GEN statistics due to averaging and regularization of the generated values. Figure 11a shows that FRT actually does not significantly change the correlation structure, but slightly decreases lnK variance and modifies the log-normal distribution close to the origin (Figure 11b). Therefore, lnK variance is 3-4% reduced for the high heterogeneity cases (σ_Y^2=6-8), but for smaller σ_Y^2 differences are negligible. Although FCT exactly reproduces log-conductivity ensemble statistics, I choose FRT in this thesis due to its computational efficiency and comparatively high accuracy. Note that FRT retains all aforementioned properties of the FCT and also shows significant advantage due to more stabilized flow solver and particle tracking algorithm.

3.4 Flow in heterogeneous porous media (paper II and III)

Figure 12 presents a multi-resolution head and streamline solution at the highest level 4 (n_j=*32*) for different resolutions of the log-conductivity field (n_Y=*4-32*; realization from

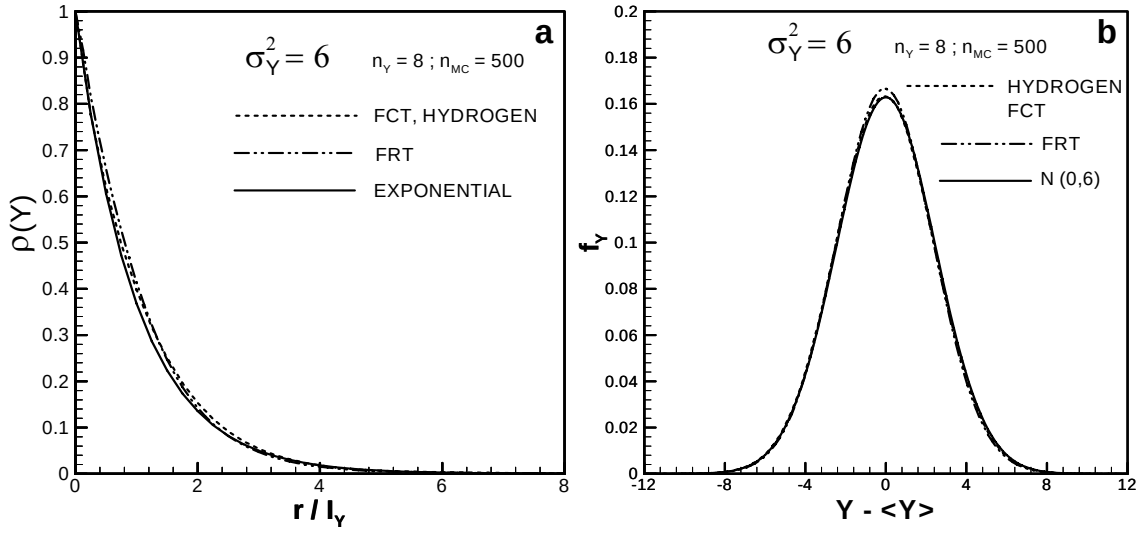

Figure 11. Log-conductivity ensemble statistics: a) autocorrelation of the log-conductivity field and b) log-conductivity pdf obtained by HYDRO_GEN, FCT and FRT using n_Y = 8, 500 Monte-Carlo realizations, exponential covariance and σ_Y^2 =6.

Figure 10; mean uniform flow). Although there are small differences between different log-conductivity resolutions, they cause small head differences, but larger streamline or velocity differences. Generally, flow or streamline patterns are similar for all log-conductivity resolutions, characterized by preferential flow channels (Moreno and Tsang, 1994), but shape, position and numbers of channels are slightly different.

Moreover, Figure 12 presents streamline fields that are obtained from the AFCM continuous velocity approximation which is necessary for accurate and reliable particle tracking that will be explored in the sequel. Relative accuracy of the velocity is lower,

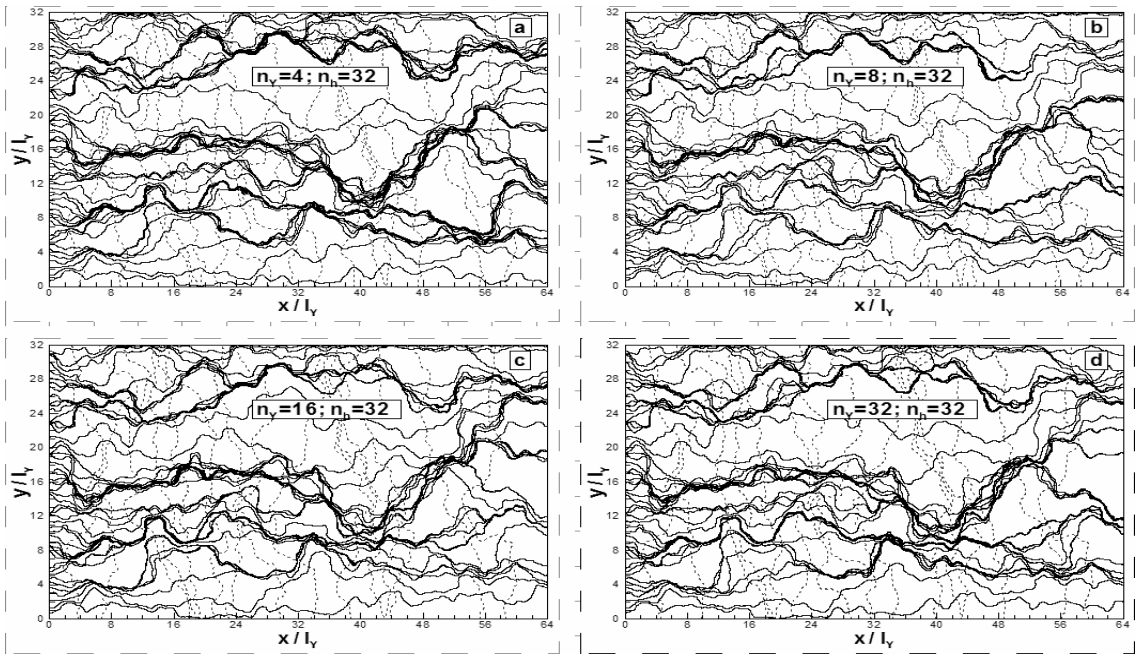

Figure 12. Multi-resolution Fup approximation of the head and streamline field (one chosen realization from the Figure 10) with exponential covariance and σ_Y^2 =6 for different resolution levels of the generated conductivity field (n_h=32 and domain is 64I_Y *32I_Y): a) n_Y=4; j=1 , b) n_Y=8; j=2, c) n_Y=16; j=3, d) n_Y=32; j=4.

around one order of magnitude compared to the head accuracy, due to strong *Fup* correlation with the polynomial type of approximation.

Velocity statistics can be described in terms of first two moments, correlations and related pdf's. Figure 13 represents mean and variance for Eulerian velocity, but also for Lagrangian velocity and their other two variants: slowness and slope. Figure 13a illustrates how different dimensionless mean velocities change with increasing σ_Y^2. Arithmetic mean of v_x/u and v_y/u is unity and zero, respectively (Dagan, 1989). Geometric mean of the dimensionless Lagrangian velocity w/u increases linearly, while Eulerian geometric mean decreases nonlinearly with increasing σ_Y^2, due to the formation of preferential flow "channels". An empirical expression for geometric mean of Lagrangian velocity suggested by Cvetković et al. (1996) appears as a good estimator, even for $\sigma_Y^2 > 4$. Note that arithmetic mean of αu and β is unity and zero, respectively. Finally, arithmetic mean of w/u is unity.

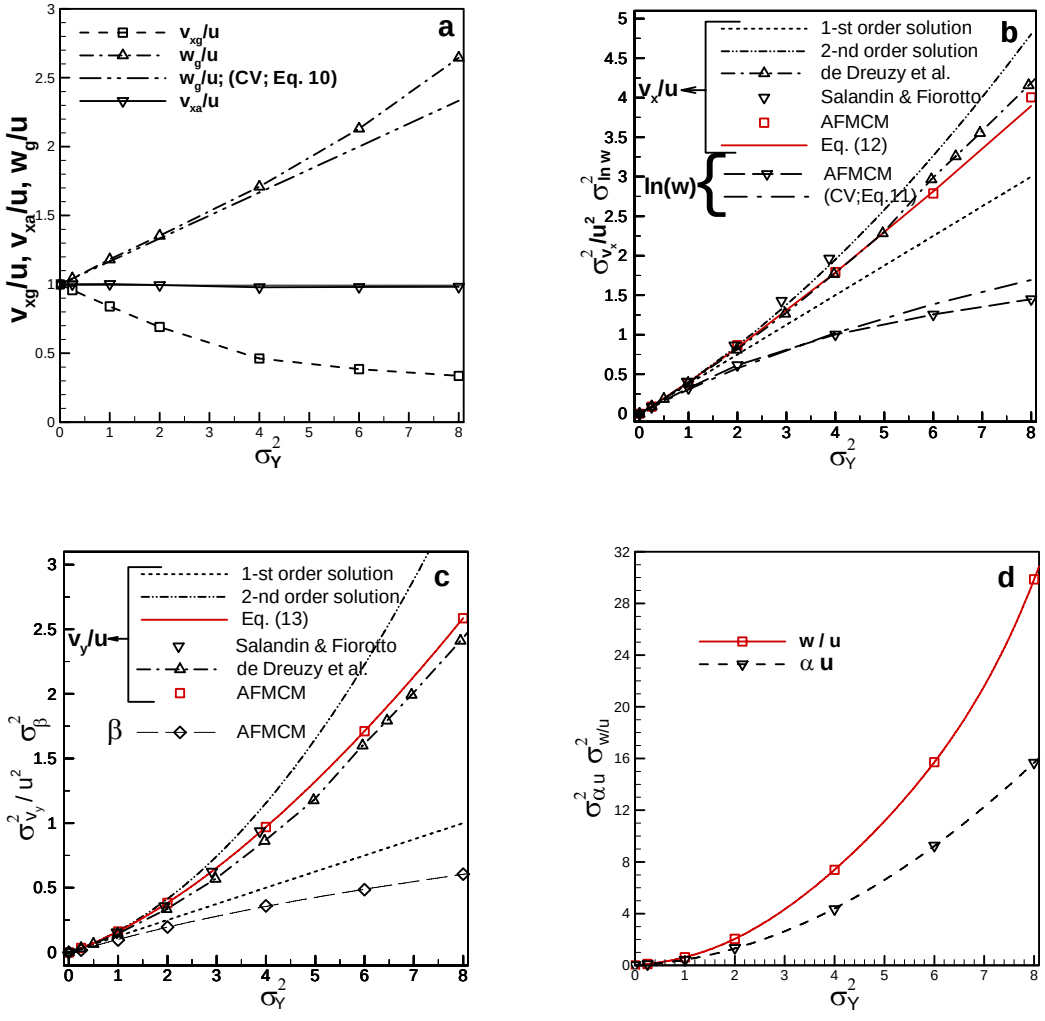

Figure 13. First two Eulerian and Langrangian velocity moments as a function of σ_Y^2 : a) Arithmetic and geometric means, variance values of b) v_x/u and ln(w), c) v_y/u and β and d) αu and w/u.

In Figures 13b-d the dependence of velocity-related variances on σ_Y^2 is illustrated. The Eulerian velocity variance is bounded by the first (Rubin, 1990) and second (Hsu et al., 1996) order results as lower and upper limit, respectively (Figures 13b-c). The first order solution is accurate for low heterogeneity cases $\sigma_Y^2 < 1$ and acceptable for mild heterogeneity with $\sigma_Y^2 \le 2$ (relative error less than 10% for longitudinal velocity, but up to 34% for transverse velocity). The second order solution is accurate and robust for low and mild heterogeneity, but not appropriate for high heterogeneity (for $\sigma_Y^2 = 4$ relative error is around 19% for transversal velocity).

Generally, both analytic solutions better approximate longitudinal than the transverse velocity variance. Numerical results of Salandin and Fiorotto (1998) agree quite well with our results up to $\sigma_Y^2 \le 4$, especially for transverse variance. Their longitudinal variance is a slightly higher than the second order theory which may be a consequence of the small numerical error. Recent numerical results of de Dreuzy et al. [2007] which used $\sigma_Y^2 \le 9$ are in a close agreement with Salandin and Fiorotto (1998) for σ_Y^2 up to 4, but they did not report results for $\sigma_Y^2 > 4$. De Dreuzy et al. (personal communication) calculated flow

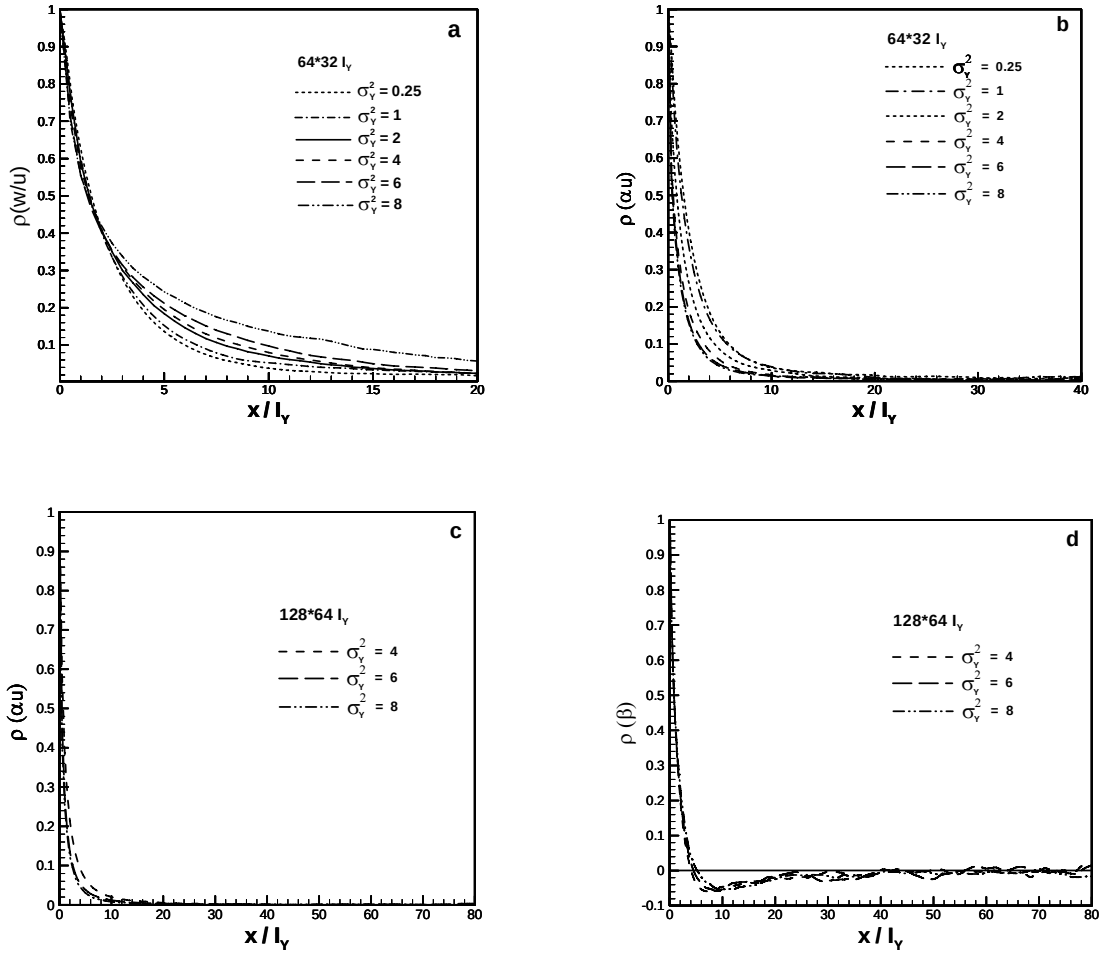

Figure 14. Correlation functions for different σ_Y^2 in the streamline longitudinal direction: a) Langrangian velocity for domain 64*32I_Y, b) slowness or inverse Langrangian velocity for domain 64*32I_Y, c) slowness for domain 128*64I_Y and d) slope for domain 128*64I_Y.

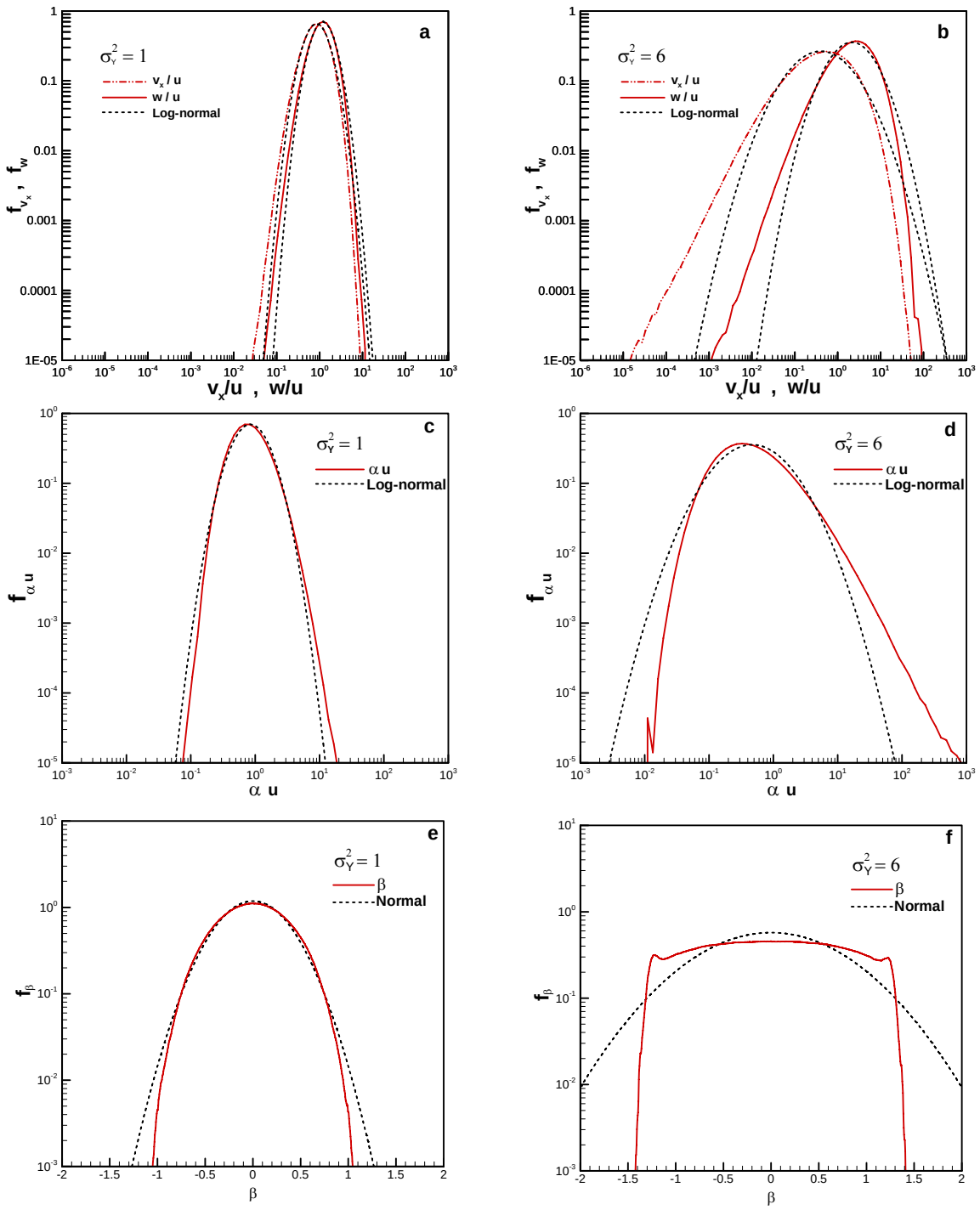

Figure 15. Velocity pdf's in log-log scale: a) Eulerian and Langrangian velocity pdf for a) $\sigma_Y^2 = 1$ ***and b)*** $\sigma_Y^2 = 6$, ***inverse Langrangian velocity or slowness (α) pdf for c)*** $\sigma_Y^2 = 1$ ***and d)*** $\sigma_Y^2 = 6$. ***Comparison with log-normal distributions is also included. Pdf's of slope (β) in semi-log scale for e)*** $\sigma_Y^2 = 1$ ***and f)*** $\sigma_Y^2 = 6$. ***Comparison with normal distributions is also included.***

statistics in a single realization of a large domain (409.6*409.6IY and nY=10). They obtained 6-8 % smaller variances than published MC results with 100 realizations (de Dreuzy et al., 2007) explaining this difference due to a lack of the extreme velocity values in the single realization. Furthermore, Zinn and Harvey (2003) reported smaller variance values than de Dreuzy et al. (2007) although they used the same block-centered finite difference procedure. Nevertheless, I can conclude that our velocity variances are in a good agreement with de Dreuzy et al. (personal communication) for high heterogeneity in a wide range of $\sigma_Y^2 \in [0,8]$. Estimators presented in paper III (their Eq. 12 and 13) appear as a robust predictor for all σ_Y^2 and both variances. Figure 13b shows dimensionless variance of log-Lagrangian velocity for which empirical expression given by Cvetković et al. (1996) appears as a good estimator, even for $\sigma_Y^2 > 4$.

Figure 13c presents variance of the slope function which is smaller than one and increases as σ_Y^2 increases due to more variable flow in transversal direction. Figure 13d presents dimensionless variances of Lagrangian velocity and slowness which are significantly larger than Eulerian velocity variances.

Figures 14a-d illustrate correlation functions of Lagrangian velocity w, slowness α and slope β, for different σ_Y^2. Lagrangian velocity correlation function increases with increasing σ_Y^2 (Figure 14a) contrary to the Eulerian longitudinal velocity component (Salandin and Fiorotto, 1998). Thus the opposing effect of increasing σ_Y^2 on the correlation function of v_x and w clearly demonstrates the effect of increasingly persistent flow along preferential channels.

Correlation of the slowness *a* decreases with increasing of σ_Y^2 (Figures 14b-c), which has direct effect on the longitudinal dispersion quantified by the travel time variance. Furthermore, travel time variance is a completely defined by the covariance of the slowness (Eq. 12). Figures 14b-c indicates a relatively small slowness correlation length and integral scale, approximately equal to the integral scale of log-conductivity. Therefore, integration of Eq. (12) yields only after a few I_Y a near linear travel time variance. After $30I_Y$, slowness correlation reaches zero for all considered σ_Y^2. The travel time variance asymptotically reaches a linear form after about $60I_Y$ due to properties of Eq. (12).

Figure 14d presents slope correlation for high heterogeneity cases $\sigma_Y^2 \geq 4$. The slope correlation shows "hole effect" with integral scale which converges to zero. Correlation does not change significantly with increasing σ_Y^2, approaching zero correlation between 4 and $5I_Y$. By definition of Eq. (12), transverse displacement variance asymptotically reaches constant sill if integral scale of the slope function converges to zero.

Eulerian and Lagrangian velocity pdf's are illustrated on a log-log plot in Figures 15a-b for a low and high σ_Y^2. The two pdf's are very close for small heterogeneity as assumed by first-order theory (Dagan, 1989), but significant differences arise for high heterogeneity $(\sigma_Y^2 > 3)$ (Figure 15b). Once again, the divergence of the v_x and w pdf's with increasing σ_Y^2 indicate preferential flow or channeling (Moreno and Tsang, 1994, Cvetković et al., 1996): The Lagrangian velocity pdf reflects a higher proportion of larger velocities pertinent to the trajectories. By contrast, Eulerian velocity pdf reflects a significant part of low velocities, since preferential flow channels occupy only a relatively small portion of the domain. Thus, differences between Eulerian and Lagrangian velocity pdf, as well as pdf deviations from the log-normal distribution are indicators of preferential flow and channeling.

Slowness (α) pdf shows similar characteristics as the Lagrangian velocity (w) pdf concerning its shape, deviations from the log-normal distribution and its tailing (Figure 15c and 15d). Slope (β) pdf shows symmetric and nearly normal distribution for low heterogeneity (Figure 15e). High heterogeneity (Figure 15f) causes strongly non-normal behavior implying a more uniform pdf and different

shape of the tailings in comparison to the normal distribution.

3.5 Advective transport based on travel time approach (paper III and IV)

Advective transport simulations are performed in the inner computational domain in order to avoid non-stationary influence of the flow boundary conditions (Figure 1). Injection tracer mass is divided to the certain number of particles which all carry the equal fraction of total mass. Particles are injected along the source line and followed downstream such that transverse displacement and travel time are monitored at arbitrary control planes denoted by x. There are two different injection modes: uniform resident and uniform in flux (Kreft and Zuber, 1978, Demmy et al., 1999). Resident mode injects particles uniformly along the source line, while in flux mode injects particles non-uniformly, i.e. proportional to the velocity field in the source. All input data are given in paper III.

The first moment of the transverse displacement η is close to zero with maximum absolute values less than $0.1 \cdot I_Y$. Figure 16a shows dimensionless transverse displacement variance σ_η^2 for all control planes and considered σ_Y^2. Variance σ_η^2 increases non-linearly with distance and its form as a function of x is in qualitative agreement with the first-order solution. The magnitude of σ_η^2 is underestimated by the first-order results with relative error of 12.8% for σ_Y^2=0.25 and 39.4% for high heterogeneity.

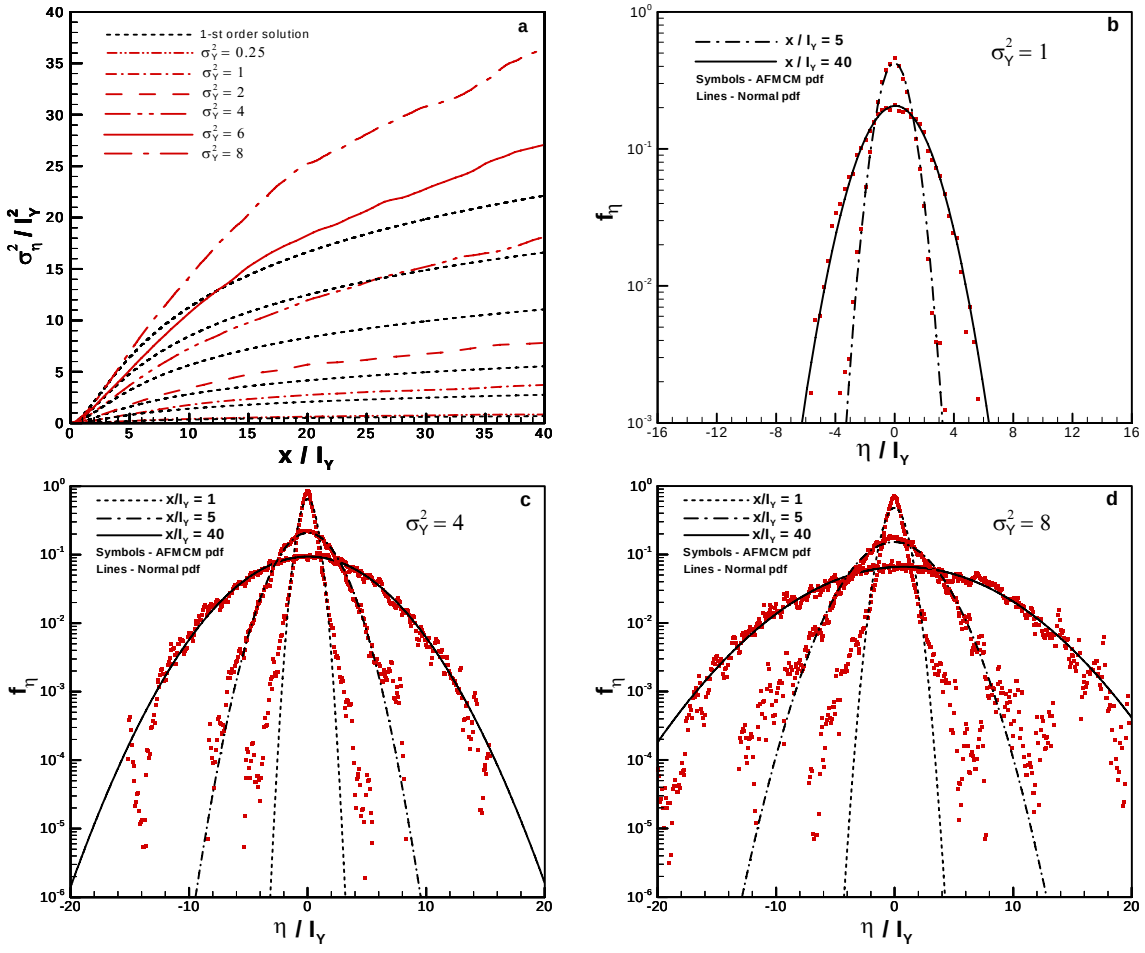

Figure 16. Dimensionless transverse displacement: a) variance for all considered σ_Y^2, pdf's in semi-log scale for different control planes and b) σ_Y^2=1, c) σ_Y^2=4 and b) σ_Y^2=8.

Figures 16b-d show transverse displacement pdf (σ_Y^2=1, 4 and 8) at three different control planes (x/I_Y=1, 5 and 40). Generally, the transverse displacement pdf shows a higher peak and wider tailings compared to the normal distribution, mainly due to streamline fluctuations around the mean and flow channeling. These deviations are more significant for very close control planes (x/I_Y<10) and high heterogeneity cases ($\sigma_Y^2 \geq 4$). Moreover, for x/I_Y>20 transverse displacement is found to be very close to the normal distribution, even in a case of high heterogeneity (Cvetković et al., 1996).

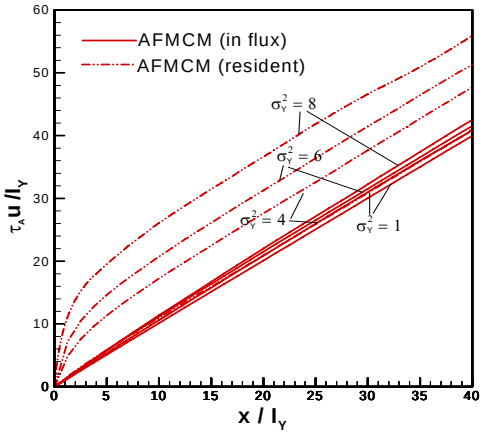

Figure 17. The dimensionless travel time mean for in flux and resident injection mode and for σ_Y^2=1, 4, 6 and 8.

The dimensionless mean travel time is presented in Figure 17. It is closely reproduced with $x' = x/I_Y$ for in flux injection mode and all considered σ_Y^2 according to the Demmy et al. (1999) and paper III. Second order prediction by Guadagnini et al. (2003) is quite accurate for low and mild heterogeneity (σ_Y^2<3) and resident injection mode. Initial nonlinearity is caused by an injection of tracer particles to the mainly low velocity zones and therefore produces larger mean travel time. However, after $5\text{-}15I_Y$ all curves become linear with nearly the same slope because particles are almost transferred and located in the preferential flow channels.

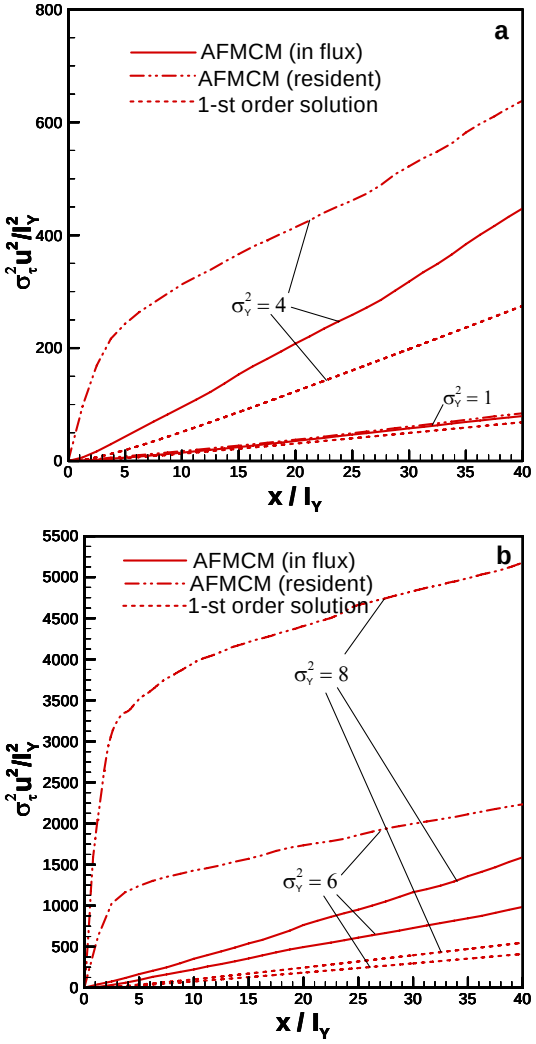

Figure 18. Dimensionless travel time variance of AFMCM and analytic solutions for: a) σ_Y^2 = 1 and 4, b) σ_Y^2 = 6 and 8.

The dimensionless travel time variance as a function of distance is illustrated in Figure 18 where a comparison is made with the first-order solution. The simulated variance for in flux mode is a nonlinear function of the distance from the source only say up to about $5I_Y$, after which it attains a near linear dependence. Interestingly, the non-linear features of σ_τ^2 with distance diminish as σ_Y^2 increases: The discrepancy of the simulated σ_τ^2 from a line set at the origin is larger for say $\sigma_Y^2 = 1$ (Figure 18a) than for $\sigma_Y^2 = 8$ (Figure 18b); this σ_τ^2 behavior was explained above with respect to the slowness correlation (Eq. 12).

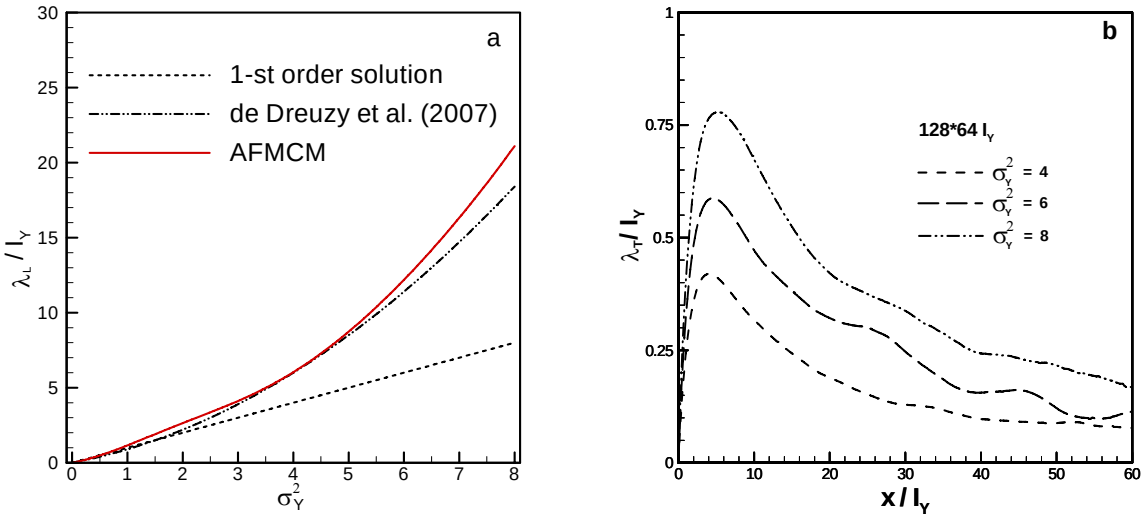

Figure 19. Asymptotic longitudinal dispersion as a function of σ_Y^2 (a). Pre-asymptotic transverse dispersion for high heterogeneity as a function of x/I_Y (b).

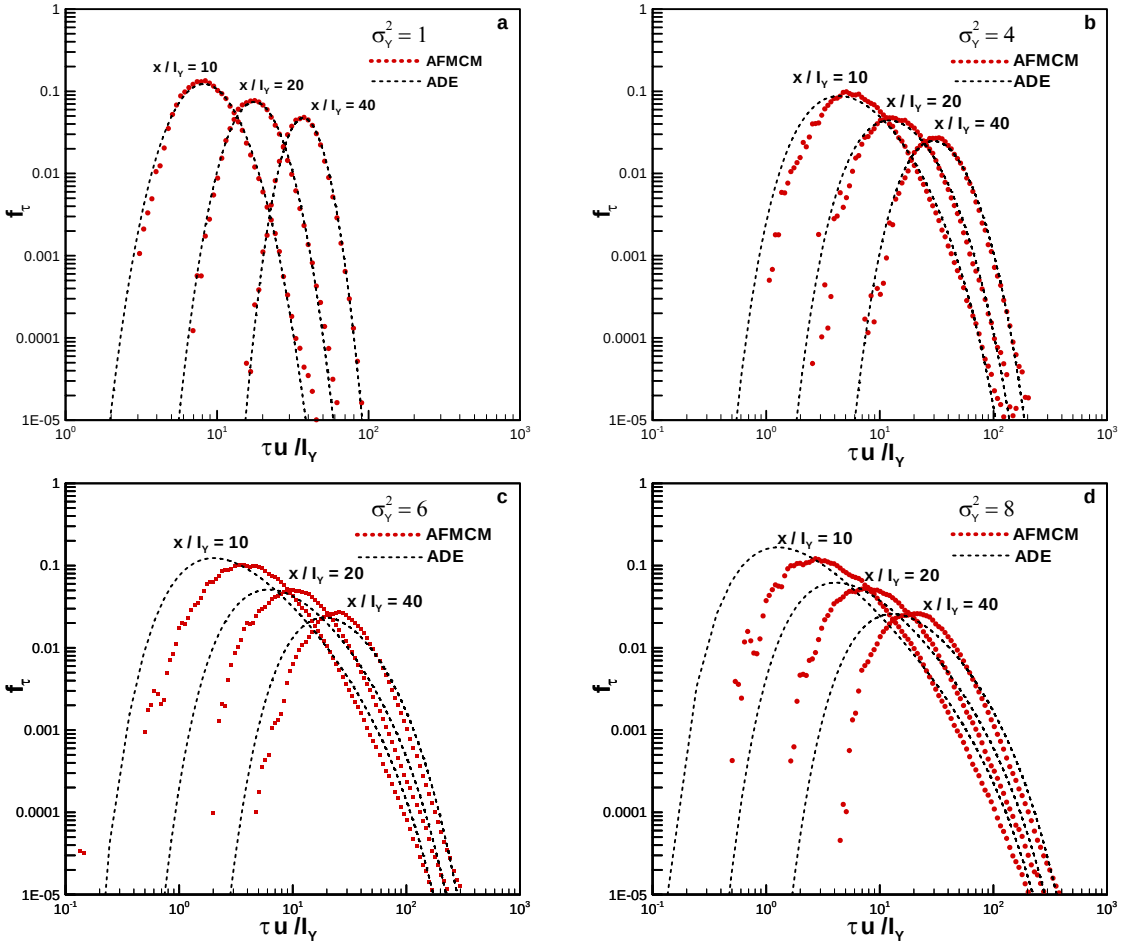

Figure 20. Travel time pdf (AFMCM and ADE solutions) for in flux mode, three different control planes and σ_Y^2 =1, 4, 6 and 8 in log-log scale.

Resident injection mode changes the form of variance from the familiar concave predicted by the first-order theory to a convex form for a case of high heterogeneity (σ_Y^2>3) according also to Cvetković et al (1996). In this case, due to tracer injection mostly to slow streamlines, slowness as well as Lagrangian velocity is non-stationary for the first *5-15*I_Y, until the particles do not reach the nearly asymptotic Lagrangian velocity which is the same as flux averaged Eulerian velocity imposed by in flux injection mode (see discussion of Le Borgne et al., 2007, 2008; paper III). The comparison with analytic solutions indicates, consistent with earlier studies, that up to $\sigma_Y^2=1$, the first-order theory reproduces simulated values reasonably well, although some deviations are visible even for $\sigma_Y^2=0.25$ (see paper III). With increasing σ_Y^2, the deviations are significantly larger, especially for high heterogeneity and resident injection mode. Consequently, all other higher moments demonstrate the same behavior for both modes and σ_Y^2 attaining the linear behavior after the first *5-15*I_Y (paper IV).

Using travel time variance and its relation with covariance of the slowness (Eq. 12), it is possible to obtain asymptotic longitudinal dispersivity. Comparison with first order theory (Dagan, 1989) and recent simulations results for normalized longitudinal asymptotic effective dispersivity of de Dreuzy et al. (2007); their average fitted curve $0.7\sigma_Y^2+0.2\sigma_Y^4$ compares reasonably with AFMCM estimator, especially for high heterogeneity around σ_Y^2=4 (Figure 19a). Small deviations occur for mild heterogeneity (σ_Y^2=1-2) and extremely high heterogeneity (relative error for σ_Y^2=8 is around 14%).

Asymptotic transverse dispersion depends only on the second moment of the slope function; more precisely on its variance and integral scale. Figure 14d shows that integral scale of the slope function converges to the zero which means that transverse macrodispersion value also goes to zero. However, I can show only pre-asymptotic behavior because asymptotic distance outperforms our current computational capacity. Figure 19b presents pre-asymptotic behavior of the transverse dispersion (flow domain 128*64 I_Y) within the first *60*I_Y in which maximum value is reached after only 4-5I_Y, followed by a decreases for $\sigma_Y^2\geq$4, but with a slower rate for increasing σ_Y^2.

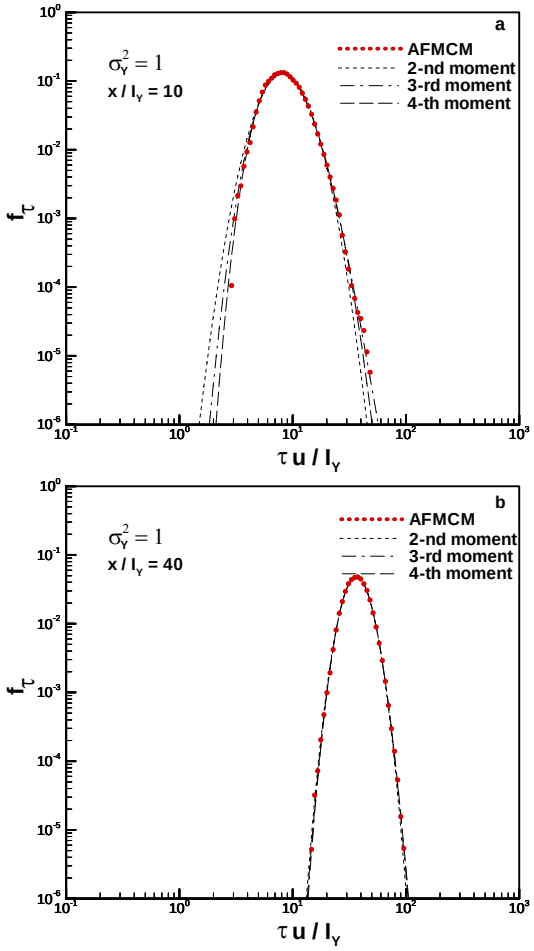

Figure 21. MaxEnt travel time pdf for in flux mode and $\sigma_Y^2=1$ using the first four travel time moments and two control planes: a) x/I_Y=10, and b) x/I_Y=40.

The travel time probability density functions (pdf's) are illustrated on a log-log plot for in flux injection mode, three chosen control planes and σ_Y^2=1, 4, 6 and 8 in Figure 20. Comparison between AFMCM and ADE (Kreft and Zuber, 1978) is also included. From low to moderate variability ($\sigma_Y^2\leq$3) inverse Gaussian pdf reproduces reasonably well the actual pdf (Figure 20a) in particular for x/$I_Y\geq$10. For high heterogeneity (σ_Y^2>3) and small distances from the source area

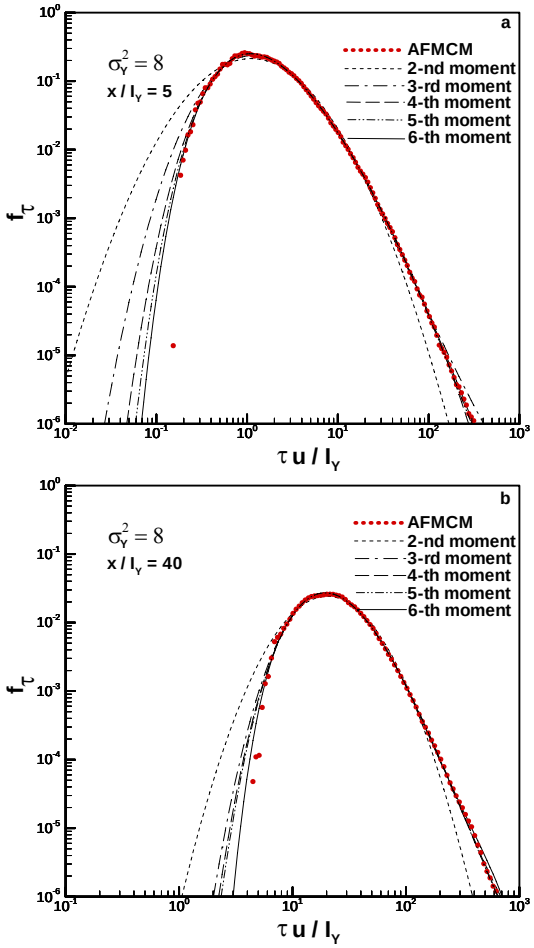

Figure 22. MaxEnt travel time pdf for in flux mode and $\sigma_Y^2 = 8$ using the first six travel time moments and two control planes: a) x/I$_Y$=5, and b) x/I$_Y$=40.

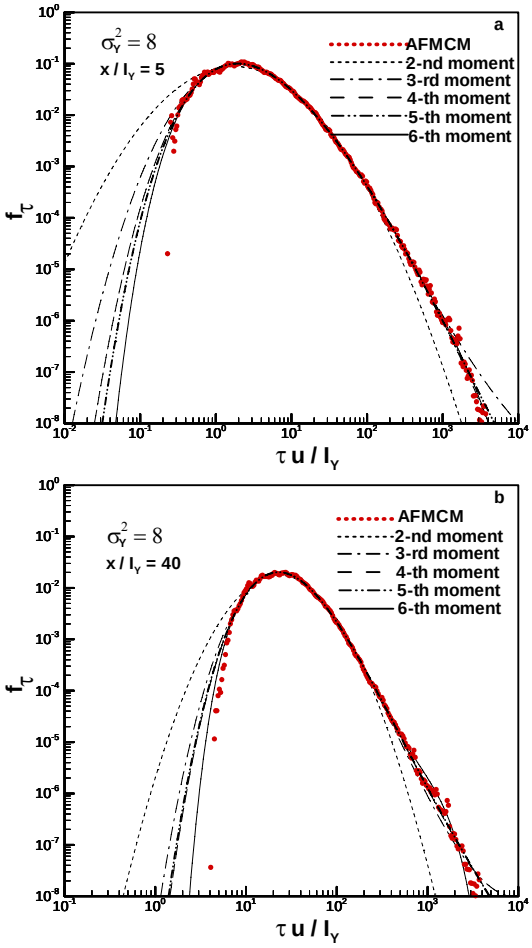

Figure 23. MaxEnt travel time pdf for resident mode and $\sigma_Y^2 = 8$ using the first six travel time moments and two control planes: a) x/I$_Y$=5, and b) x/I$_Y$=40.

($x/I_Y \leq 20$) inverse Gaussian pdf deviates from the simulated pdf in the first part of the breakthrough curve.

However, with increasing distance, the difference between simulated and modeled curves decreases, while after around $40I_Y$ the inverse Gaussian pdf reproduces well the peak and later part of the experimental pdf (Figure 20b-d). Therefore, advective transport in highly heterogeneous porous media is a non-Gaussian for the first $40I_Y$.

Figures 21-23 show the Monte-Carlo experimental AFMCM pdf as well as its MaxEnt approximation pdf (paper IV) which uses the travel time moments up to the 6-th order, both modes, different control planes and σ_Y^2. Generally, deviations from a symmetrical distribution (e.g., log-normal) or MaxEnt pdf with first two moments decrease with distance from the source area, and increase significantly with increasing σ_Y^2.

For low and mild heterogeneity (for instance σ_Y^2=1, in flux mode, Figure 21) small deviations from a symmetric distribution occur only within the first 10-20 integral scales, while almost complete symmetry is attained after 40 integral scales. It means that the higher travel time moments only slightly change pdf close to the source area. Furthermore, this is very strong evidence jointly with paper III (see their Figure 2 and pdf results for σ_Y^2=0.25) that the first order theory presents robust and efficient tool for

travel time analysis in low heterogeneous media ($\sigma_Y^2<1$) where mean and variance completely describes advective transport. For mild heterogeneity ($1\leq\sigma_Y^2\leq3$) asymmetry of the travel time pdf becomes larger, while the first order theory is only partially adequate due to variance error (see paper III). Mild heterogeneity range presents a transition zone where the higher travel time moments start to play a more important role. Pdf results for resident mode are practically the same due to similar travel time moments (Figures 17-18).

For high heterogeneity and in flux mode (e.g. $\sigma_Y^2=8$, Figure 22) the computed AFMCM pdf is increasingly asymmetric, with both the early and late arrivals are shifted to later times with respect to the log-normal pdf (MaxEnt with two moments). Although the asymmetry in the pdf diminishes with increasing distance, for high heterogeneity it is still maintained over the entire considered domain of 40 I_Y. Generally, the main influence has the third moment which represents pdf skewness. Four and other higher travel time moments only improve MaxEnt pdf with respect to early arrivals, but peak and last arrivals remain almost the same.

Figure 23 presents that travel time pdf for very high heterogeneity case with $\sigma_Y^2=8$ and resident injection mode requires between three and four moments for both: peak and late arrivals. Late arrivals in resident injection mode depend on certain number of particles which considerably slow down in the low conductivity zones due to injection and needs long time to come into the preferential flow channels. Therefore, pdf of the resident injection consists of significantly longer tailing than in flux mode and therefore requires additional fourth moment for its accurate describing.

4 DISCUSSION

Since detailed field experiments are very rare, the scarcity of data and uncertainty of input and output variables mean that stochastic computational methodologies are usually key tools in explaining complex subsurface processes. Even in rare cases, for instance the Cape Cod site (*LeBlanc et al.*, 1991), it is impossible to completely reduce uncertainty and get a complete deterministic description of flow and transport in porous media. Unfortunately, it is not realistic to expect that we will find some futuristic type of scanner that can accurately measure all heterogeneous physical and chemical properties of porous media and precisely record the movement and behavior of the flow and solute transport. However, even in that unrealistic case, computational methodologies represent the only way to scientifically describe and explain these recorded subsurface processes. Finally, and more realistically, different computational methodologies need to describe subsurface processes while honoring the intrinsic uncertainty in our analysis.

It has already been discussed in the Introduction that there is no universal methodology that solves all subsurface problems. This thesis tried to develop a novel computational approach that is based on atomic basis functions, respects the multi-resolution nature of measurements and their physical interpretation and enables an adaptive and accurate procedure that can work with different numerical and stochastic approaches and be applied to many different subsurface processes. Therefore, this section will discuss properties of the methodology and its particular application to groundwater problems with sharp fronts as well as to single-phase flow and advective transport problems presented in this thesis. Furthermore, some attention will be devoted to future advancements and improvements that are possible based on the results of this thesis.

4.1. An adaptive multi-resolution methodology

In this thesis, different computational tools are developed based on adaptive multi-resolution methodology, such as Fup transformations for multi-resolution representation, AFCM for flow problems and tracking of solutions with sharp fronts, AFMCM for stochastic modeling of flow and advective transport and IFMEA for statistical description of Monte-Carlo or other related pdf´s in terms of a few first statistical moments. The presented methodology is appropriate for many types of subsurface processes. Therefore, this subsection will discuss atomic basis functions, general properties of the methodology and its relation to other methodologies.

4.1.1 Atomic basis functions

Atomic basis functions with compact support are the heart of the presented methodology because all of their properties are closely related to the properties of basis functions. Indeed, practically all other numerical and stochastic methods are closely related to the basis functions. Consider the following two typical examples: a) the multi-scale finite element method is completely described by multi-scale basis functions that are defined on a coarse grid, incorporating as much fine-scale heterogeneity as possible and b) the maximum entropy algorithm, based on orthogonal polynomials, shows significantly better numerical properties than if it provides monomials as basis functions.

Atomic basis functions have a strong mathematical background as the exact solutions of differential-functional equations (14). In principle, each type of atomic basis function is related to a particular linear differential operator. This means that, theoretically, each problem can be exactly defined by certain types of atomic basis functions. However, the mathematical theory for defining atomic basis functions is not so simple and straightforward, and special cases have been developed that exactly describe algebraic (Fup_n), exponential (y_ω) and trigonometric ($y_{\omega,h}$) polynomials. Since all possible mathematical solutions can be represented by combinations of only these three basic polynomials, the main idea behind the presented methodology is to use certain types of atomic basis functions that directly span the solutions (its vector space) of some particular problem. In that way, computational methodology becomes

optimal and efficient due to the small number of basis functions used, and it also creates synergy between mathematical and physical interpretations.

The most commonly used basis functions in computational sciences are algebraic polynomials or functions that exactly describe them, such as splines, wavelets or Fup_n basis functions. It is interesting to note that there have been only a few attempts with non-classic choices such as radial basis functions (e.g., Kansa, 1990). The reason for that lies in the simplicity of algebraic polynomials, which are easy to use on the computer and have a long history. Thus, scientists try to find new techniques only if they cannot solve new physical challenges with old methods. This is one of the reasons why the finite element methods are still the most frequently used computational technique in applied science. Furthermore, in this thesis Fup_n basis functions are used, which are also closely related to the algebraic polynomials. However, these functions are the most widely known atomic functions with well-defined properties, and they provide a solid foundation for the methodology and applications proposed in this thesis. Nevertheless, I believe that future applications of other atomic basis functions will significantly improve the ability to solve some subsurface problems. In order to show such potential applications, the 1-D steady-state advection dispersion equation is considered

$$\frac{\partial^2 c}{\partial^2 x} - Pe\frac{\partial c}{\partial x} = 0 \tag{41}$$

where $Pe = v_x / D$ is the Peclet number, and c(0)=0 and c(1)=1 are the Dirichlet boundary conditions. The exact solution is

$$c(x) = \frac{\exp(Pe\,x) - 1}{\exp(Pe) - 1} \tag{42}$$

This solution is characterized by a sharp front at the right boundary if the Peclet number is high. For Pe=1000, the AFCM requires a few hundred Fup_n basis functions, while only a few exponential basis functions are needed for the exact solution with frequency equal to the Peclet number (y_{1000}). This simple example shows that appropriate basis functions can dramatically reduce the computational burden. Moreover, the Peclet number as a measure of the relation between advection and dispersion is the key parameter (frequency) of the exponential basis function. It means that each physical problem has a simple mathematical solution (in spirit of Einstein, 1905), but achieving this is sometimes more art than science. The real question remains whether it is better to find a bad solution with an old approach many times or a good solution with a new approach only once. My opinion is that many computational methods possess inherent problems, mainly due to forcing classic basis functions for all possible physical problems. In the following, some relevant properties of the presented methodology, which uses Fup basis functions, will be discussed.

4.1.2 General properties

The main properties of the Fup methodology presented in this thesis are: 1) computational capabilities of Fup basis functions with compact support, 2) multi-resolution presentation of heterogeneity as well as all other input and output variables, 3) accurate, adaptive and efficient strategy and 4) semi-analytical properties.

Fup basis functions, wavelets and splines are similar mainly due to their compact support and possible numerical implementation. Generally, approximation properties of all these basis functions are related to the development of algebraic polynomials. *Fup* and other atomic basis functions can be regarded as generalized splines of infinite smoothness C^∞ (Rvachev, 1982). In the spirit of wavelet and multi-resolution analysis, atomic basis functions can be regarded as scaling functions that enable a direct relationship with wavelets (Mallat, 1989). It should be noted that the importance of the atomic function *up(x)* in the functional-theoretical sense follows from its "atomic role" in the space of C^∞ functions, which is similar to that played by wavelet functions in the space $L^2(R)$. Kravchenko et al. (1995) developed wavelet basis functions with aid of the atomic basis functions, consisting of superior approxima-

tion properties in comparison to other known wavelet functions.

The basic difference between *Fup* and atomic basis functions on the one hand and wavelets and splines on the other hand is that, generally, atomic basis functions present exact solutions of differential-functional equations, but splines and wavelets are obtained from particular types of mathematical transforms. This is the reason why *Fup* basis functions have an infinite number of derivatives and non-vanishing moments. Therefore, *Fup* and atomic basis functions are appropriate for efficiently solving boundary-initial value problems as well as for designing promising new mesh-free numerical approaches.

Fup basis functions support multi-resolution analysis originally developed by wavelet basis functions that enables representation of all spatial and temporal scales for flow and transport variables. This is particularly important for log-conductivity heterogeneous fields and the contribution of different scales to head, velocity or travel time ensemble statistics. Furthermore, sparse measurements are usually obtained on different scales. It is very important to incorporate all measurements with original scales for a more reliable estimation of flow and transport in porous media.

The main computational idea behind this approach is to separately find the minimum number of basis functions and resolution levels necessary to describe each flow and transport variable with the desired accuracy on a particular adaptive grid. Therefore, each variable is separately analyzed, and the adaptive and multi-scale nature of the methodology enables not only computational efficiency and accuracy, but it also describes subsurface processes closely related to their understood physical interpretation. The methodology inherently supports a mesh-free procedure, avoiding the classical numerical integration, and yields continuous velocity and flux fields, which is vitally important for flow and transport simulations.

Thus, all variables and ensemble statistics are described only by a few basis functions (Eq. 26) and the appropriate Fup transformation (e.g., FCT or FRT). Therefore, final ensemble statistics can be regarded as semi-analytical solutions because they are represented only by a finite number of Fup basis functions obtained with the prescribed accuracy. These solutions can be transformed into any appropriate relation with standard mathematical functions. For example, paper III presented MC ensemble solutions for Eulerian velocity variance, travel time variance and longitudinal macrodispersivity. Moreover, the travel time pdf in paper IV is simply represented by the analytic form of the maximum entropy pdf. These results can be regarded as semi-analytical solutions as well as many other first-order perturbation results, especially because they use a significantly smaller number of approximations and assumptions.

4.1.3 Relation with other numerical methods

The presented methodology (AFCM) combines the most desirable properties of existing numerical methods: 1) localized basis functions as in conventional FE, 2) the application of a strong formulation and simple procedure as in conventional FD, 3) accuracy and continuity of basic variables and their derivatives and the use of Fup transformations as in spectral methods, and 4) adaptive and efficient procedures with error estimation as in all modern numerical approaches.

Paper II presented a flow solver in heterogeneous porous media and discussed its advantages and disadvantages in relation to other common numerical methods. MODFLOW (McDonald and Harbouch, 1988) is still the most simple, but also the most reliable, flow solver. AFCM offers a multi-resolution description of heterogeneity in a more transparent way and enables adaptive and more accurate solutions than MODFLOW (especially for the velocity field), but it requires a more expensive flow solver and a higher head resolution level than lnK field. The main reason for this inefficiency in terms of the number of head unknowns lies in the collocation nature of the algorithm, which does not exactly satisfy mass balance. One possibility for further improvement is the Fup Galerkin method, made through the weak integral formulation, which would keep all mentioned

AFCM properties but also ensure exact mass balance on compact support.

Presented methodology is currently not suitable for the description of irregular geometries. Irregular geometry can be solved by R-functions, or Rvachev functions—a special numerical framework that exactly describes boundary conditions on domains with irregular boundaries independently on atomic basis functions (Rvachev et al., 2000; Tsukanov and Shapiro, 2005). Furthermore, a combined algorithm of R-functions and atomic basis functions could be a particularly efficient methodology that uses R-functions for the exact treatment of boundary conditions, while the chosen atomic basis functions use an adaptive strategy that accurately describes the solution inside the domain.

The FE and FV methods eliminate this geometry problem but have the inherent disadvantage that in order to produce the continuous velocity field needed for reliable random walk methods, they require velocity postprocessors, hybrid formulations and additional CPU work. A recent new formulation of MsFEM (Hou and Wu, 1997) tried to obtain a continuous velocity field on a coarse grid by utilizing the fine-scale heterogeneity effects through the multi-scale coarse basis functions. Unfortunately, all these methods, including the AFCM, require a very fine grid and extensive computational resources, especially for larger lnK variance. In order to obtain more efficient flow solutions in heterogeneous porous media and retain the accuracy of the AFCM, the computational strategy should definitely be changed. From the perspective of atomic basis functions, a promising approach could use exponential basis functions. The key task is to define the frequencies of basis functions with respect to heterogeneity variations of the log-conductivity field. This means that heterogeneity properties directly define the characteristics of basis functions, which can significantly decrease number of basis functions and improve the efficiency of the flow solver.

Eulerian transport analysis with the advection-dispersion-reaction equation (4) is usually influenced by numerical dispersion if classic numerical methods are applied. Paper I presented the AFCM, which supports the method of lines and very efficiently tracks sharp fronts or narrow transition zones, resolving all spatial and temporal scales via an adaptive grid. Moreover, this method is closely related to wavelet methods (e.g., Vasilyev and Bowman, 2000) and does not show any sensitivity to numerical dispersion, even in a case of a high Peclet number. An adaptive grid with *Fup* basis functions finds frequencies of solution in the principally same way as exponential atomic functions used that frequencies for their construction.

Particle-tracking and random-walk methods inherently eliminate numerical dispersion, following particles according to the continuous velocity field. The presented adaptive Fup methodology (paper II) enables very efficient tracking of particles due to its accurate velocity fields and the use of Fup transformations, which can follow an unlimited number of particles with prescribed accuracy. Thus, the presented methodology has many advantages over existing procedures, but it also opens many other possibilities for developing promising new methodologies that could solve the mentioned problems in fundamentally different ways.

4.1.4 Relation with other stochastic methods

The Monte-Carlo method is still the best-known stochastic methodology for flow and transport in heterogeneous porous media. The AFMCM presented in paper II improved MC methodology based on advancements discussed in the last subsection, particularly as they apply to high heterogeneity and advective transport (papers III and IV). However, the basic problem for MC methods is that each flow realization must deal with large heterogeneity variations, which is challenging for all existing methods, as discussed earlier. Even the adaptive strategy of AFMCM cannot significantly improve the efficiency of the flow calculations, especially if heterogeneity is defined in the classic way, with the finite variance and integral scale statistically uniformly distributed throughout the domain (as in this thesis and similar generic studies). I currently see the possibility for development of more efficient methodologies in two prin-

cipally different ways: a) using totally new numerical approaches in each realization, as Janković et al. (2003) with AEM or mentioned promising methods with exponential atomic basis functions, and b) providing new stochastic methods that directly solve ensemble statistics (pdf and related moments). Two such novel stochastic methods are PCM (Zhang and Lu, 2007; Shi et al., 2009) and BME (Christakos, 2000).

PCM presents the log-conductivity field in terms of the Karhunen-Loeve (K-L) expansion and reduces a stochastic problem to many decoupled deterministic problems of the same form as the original equations (3) or (4). In that way, PCM is conceptually similar to MC methods, but it requires fewer deterministic solutions or "realizations" for each set of collocation points. However, each deterministic equation is still very demanding, with the same discussed problems, and the presented methodology can be applied as in the MC case. Also, K-L expansion is not currently developed for non-Gaussian and other arbitrary heterogeneity structures.

BME uses two strong stochastic tools: the Bayesian conditioning and maximum entropy principle. The first step in BME for finding a prior pdf can also be used for stochastic modeling of flow and transport based only on epistemic knowledge, including not only differential equations (3) and (4) but also many other types of physical laws (empirical relationships, histograms, moments and so on). This theoretically very sound approach very easily incorporates soft and hard data and different relations and directly yields pdf results. However, computational implementation is still complicated due to multi-dimensional integrals and high nonlinearity. Paper V presented the first application of the maximum entropy algorithm (IFMEA) with Fup basis functions for solving a univariate pdf. The IFMEA is used for complete characterization of the travel time pdf, combining MC analysis and the MaxEnt principle (paper IV). The possible extension of the algorithm to the multivariate pdf and combination of Fup multi-resolution approach with versatile BME properties could lead to a more computationally efficient stochastic methodology. More specifically, moments of differential equations (3) and/or (4) are zero and can be transformed into multi-dimensional Fup moments. Then, the IFMEA presented in paper V would be extended to multi-dimensional problems in order to obtain the final multivariate pdf.

4.2 Flow in heterogeneous porous media

Contrary to transport analysis, which is usually linked with many different concepts, computational frameworks and theories, the flow problem in heterogeneous porous media, as the most demanding Monte-Carlo step, is conceptually straightforward but computationally extremely difficult, as was discussed in the last subsection. Challenges for all current flow solvers include problems with: 1) complex flow regimes, 2) relatively large lnK variance and high heterogeneity, 3) 3-D large domains with irregular boundaries and 4) non-Gaussian heterogeneity structures. The presented adaptive Fup methodology (AFMCM, papers II-IV) was concentrated mainly on the second problem in this thesis. Paper I also discussed multiphase flow and density-driven flow, but in homogeneous porous media. Last two problems are very important for real applications, field experiments and tracer tests, because usually only 3-D analysis can capture many flow and transport effects (Janković et al., 2003, 2009), while real heterogeneous structures often contain connected low and/or high conductivity zones, which means that they are rarely multi-Gaussian (e.g., Gomez-Hernandez and Wen, 1998). Unfortunately, extensive 3-D simulations are very demanding and sometimes outperform even existing parallel supercomputer capabilities and computationally present an open problem due to a large linear system of equations ($O(10^9\text{-}10^{11})$).

Flow statistics in low and mild heterogeneity are similar for Eulerian and Lagrangian velocities. The most important consequence of the high heterogeneity is a change in the flow patterns in the form of preferential flow channels, which is reflected by a significant difference between the Eulerian and Lagrangian velocities (Figure 15a-b). Preferential

flow channels connect highly conductive zones and concentrate the main portion of the flow rate to a few flow paths. Therefore, Lagrangian velocity records the higher values, in contrast to the Eulerian velocity, which contains a significantly larger fraction of low velocities (paper III; Cvetković et al., 1996). Both pdfs exhibit strongly non-log-normal behavior for high heterogeneity.

High heterogeneity also introduces significant changes to the correlation structure of all Eulerian and Lagrangian flow variables (v_x, v_y, w, α and β). For example, v_x, w and α have essentially the same correlation structure for low heterogeneity. High heterogeneity strongly affects the correlation structure for v_x, w and α due to increasingly dramatic meandering and consequently decreases the correlation length and integral scale, except for the Lagrangian velocity w*,* which attains a non-zero correlation over many log-conductivity integral scales due to persistency of channeling. On the other hand, v_y and β show the 'hole effect', and its integral scale in the longitudinal direction converges to zero. Furthermore, correlation of the slowness, slope and its integral scales determines asymptotic dispersion behavior and plays a key role in advective transport, as quantified by the travel time approach (Dagan et al., 1992).

4.3 Advective transport

In this thesis, application of the AFMCM and its abilities were presented mainly to completely describe advective transport in heterogeneous porous media under mean uniform flow. In this subsection, the main properties of advective transport results, presented in the third section, will be discussed.

4.3.1 Transverse displacement

It has been found that transverse displacement is normal for low heterogeneity under the first-order framework (Dagan, 1989). Due to the accuracy and robustness of the presented methodology, simulations showed that transverse displacement is not normal for distances close to the source. For $x/I_Y>20$, transverse displacement was found to be very close to the normal distribution, even in a case of high heterogeneity (paper III). Therefore, kurtosis is relatively high for very close control planes, implying a sharper peak around the mean, while for $x/I_Y>20$, kurtosis is close to 3, implying convergence to the normal distribution.

4.3.2 Travel time

Since transverse displacement becomes nearly normal after only $x/I_Y=20$, even for high heterogeneity, travel time shows more complex behavior depending on the injection mode, heterogeneity level and influence of the higher moments (papers III and IV*)*.

These results show that all travel time moments beyond a certain distance from the source or injection control plane are linear. The most important reason for the initial non-linearity is the influence of the injection mode, where in flux injection preserves the linearity due to direct injection of tracer into the preferential flow channels, since the resident injection mode has a strong initial nonlinearity within the first $5I_Y$ for high heterogeneity due to the injection of the greatest number of tracer particles into the slow streamlines, which requires that distance to transfer them to the preferential flow channels.

The combination of Monte-Carlo simulations and the MaxEnt principle enables the experimental pdf to be described by only a few first travel time moments in the form of the MaxEnt pdf (papers IV and V). Particularly, the MaxEnt pdf enables an analysis of three basic parts of the travel time pdf: peak and early arrivals, which are important for risk assessment, and late arrivals, which are needed, for instance, for remediation. Generally speaking, mean and variance completely describe the travel time pdf for $\sigma_Y^2<3$, skewness is dominant for $\sigma_Y^2=4$, and kurtosis and the fifth moment are needed for $\sigma_Y^2=6$ and 8. The resident injection mode requires more moments due to the initial nonlinearity of the travel time moments. It is particularly true for late arrivals, which require the fourth moment for $\sigma_Y^2=6$ and 8. Therefore, for description of the peak and late arrivals, the most important moment is the third mo-

ment, which means that high heterogeneity mostly changes the skewness of the travel time pdf.

Since early arrivals require more moments than other parts of the travel time pdf, they are also related to the largest uncertainty with respect to the maximum entropy principle. Early arrivals predicted by the MaxEnt pdf are always shorter than the first arrivals calculated by the AFMCM, which is positive and conservative from a risk assessment point of view. Indeed, the actual error is small relative to the mean travel time. For example, the difference between first arrivals predicted by the AFMCM and MaxEnt with four moments relative to the mean travel time is less than 3% for all cases and modes (Table 4 in paper IV), which means that four moments quite accurately describe the early arrivals and significantly reduce estimation uncertainty.

4.3.3 Macrodispersion and Fickian transport

Detailed analysis of advective transport in multi-Gaussian fields enables the determination of two basic terms of classic stochastic theory: macrodispersivity and Fickianity.

Advective transport is Fickian if the longitudinal dispersivity after a sufficiently long time or distance tends to a constant value, which is usually called macrodispersion. This is required, but not a sufficient condition for Fickianity. Paper III developed the connection between slowness correlation and travel time variance, the slope of which can define longitudinal macrodispersion. The correlation of slowness decreases with increasing σ_Y^2, implying that after a $60I_Y$, the travel time variance attains a linear shape and reaches asymptotic longitudinal dispersion, given by the following empirical relationship (paper III, Figure 19a)

$$\frac{\lambda_L}{I_Y} = \left(\frac{\sigma_Y^2}{4} + \frac{\sigma_Y^4}{5} + \frac{\sigma_Y^6}{500} \right) \left(\frac{4}{3} + \frac{3}{2} \exp\left(-\frac{1}{5} \sigma_Y^4 \right) \right) \tag{43}$$

Moreover, for high heterogeneity, after only a few integral scales variance attains a near-linear shape, without indications of anomalous transport. On the other side, transversal macrodispersivity is related to the correlation of beta, which requires a considerably larger distance, so that its value converges to zero as predicted by perturbation theories (e.g., Hsu et al., 1996) and MC simulations (de Dreuzy et al., 2007) for 2-D cases. However, Janković et al. (2009) proved using simulations that in 3-D domains the transversal macrodispersivity is considerably smaller than the longitudinal, but greater than zero. They defined such mixing as a special type of "advective mixing" due to streamtube stretching, which is not present in two dimensions, showing that some effects are only visible in a real 3-D domain.

Advective transport is Fickian if mass distribution through the control plane satisfies ADE with constant longitudinal dispersivity. This is additional, sufficient condition for Fickianity. Since for instantaneous injection mass distribution is proportional to the travel time pdf, results show that advective transport for low and mild heterogeneity becomes Fickian after the first $40I_Y$, proving the robustness of the first-order theory. However, advective transport is non-Fickian for a long distance in the case of high heterogeneity. Paper IV showed that in the limit ($x/I_Y \to \infty$), the travel time pdf can be described by only the first two moments and also coincides with the ADE solution (Kreft and Zuber, 1978). In the limit, advective transport in a multi-Gaussian field converges to Fickian transport.

4.4 Other transport issues

This subsection will discuss a few transport issues that are important for applications and may be successfully solved and/or verified by the presented adaptive multi-resolution approach.

4.4.1 Field scale experiments and related heterogeneity structures

Despite the usual scarcity of data and inevitable presence of the uncertainty, field experiments are still very important for real applications as well as theoretical and computational developments. The key task for a real field experiment is to collect all possible data, including different hard and soft data such as core measurements, pumping and injection

tests, as well as usually soft geophysical data such as electrical resistivity, spontaneous potential or seismic records, geological reports or even expert judgments in order to characterize heterogeneous porous media as well as possible. Moreover, different non-reactive and reactive tracer tests give different measurements of concentration, fluxes or travel times. In that way, computational simulations can relate heterogeneous effects and output results, improve heterogeneity characterization using inverse modeling and correlate hard and soft data in order to decrease the number of measurements in the next experiment or investigate different transport concepts to correctly match experimental and simulated data. Finally, the presented methodology should be applied in new or existing field experiments in order to attain some of these goals.

Most related studies (including this thesis) discuss flow and transport in multi-Gaussian heterogeneity structures that are completely characterized by the first two moments and their lack of correlation of low and high conductivity values. Many field experiments show that multi-Gaussian fields may not be realistic, mainly due to neglect of significant correlations between highly connected zones [e.g., MADE-1 and MADE-2 tracer test; Boggs et al., 1992]. Moreover, the differences between multi-Gaussian and some selected non-Gaussian fields are discussed with respect to the travel time [Gomez-Hernandez and Wen, 1998], macrodispersion [Wen and Gomez-Hernandez, 1998], mass transfer [Zinn and Harvey, 2003] and especially the influence of the highly connected conductivity zones on flow and transport analysis [Zinn and Harvey, 2003, Liu et al., 2004, Knudby and Carrera, 2005]. Particularly, Gomez-Hernandez and Wen [1998] and Zinn and Harvey [2003] argued that first arrivals can be ten times faster in non-Gaussian fields, which are important for risk assessment, for instance. Moreover, Wen and Gomez-Hernandez [1998] proved that even in a case of low heterogeneity, macrodispersion could be considerably different in non-Gaussian fields. Furthermore, the presented methodology, due to its accuracy and generality, can resolve all flow and transport properties in non-Gaussian structures in a similar way as for multi-Gaussian fields, including fractal fields, bi-modal heterogeneity and structures with connected low and/or high permeability zones.

4.4.2 Pore-scale dispersion

Apart from advective transport influenced by velocity variations due to heterogeneity of porous formations, pore-scale dispersion (PSD) is always present and can be the dominant transport force under certain conditions. The advective velocity field pulls and stretches the solute plume by conveying the released mass through lenses and fingers of higher velocities. This process creates the concentration or solute flux gradient, along which the PSD acts as a diffusion process, diluting high concentrations and fattening the lenses and fingers (Andričević, 2008). As transport time progresses, these two processes balance each other at some effective scale. Although the Peclet number is usually high, values between 100 and 10,000 cause that PSD significantly changes the plume spreading. Since first-order analysis decouples the advective and dispersive displacements (e.g., Fiori and Dagan, 2000), random-walk simulations simultaneously follow particles with advective and dispersive steps that are modeled as Gaussian random processes (e.g., Kinzelbach, 1988, Le Bolle et al., 1996). Random-walk simulations in the presented AFMCM can potentially resolve the influence of the PSD on concentration and solute flux pdf and its higher related moments. These simulations also provide the possibility of simulating the relationship between the PSD and higher travel time moments. Finally, these MC random-walk simulations can resolve the influence of the PSD in high heterogeneity formations and verify the assumptions in the recent model of Andričević (2008), which very efficiently finds all concentration moments in a recursive way.

4.4.3 Reactive transport

Paper I shows that the AFCM inside the method of lines is well suited for problems of reactive transport, which are usually faced with sharp fronts, many spatial and temporal

scales, high nonlinearity and many variables. Each variable is defined on a particular adaptive grid with a prescribed threshold, enabling a very efficient computational approach. Reactive transport can be defined in an Eulerian framework utilizing the coupled classic advection-dispersion-reaction system of equations of type (4) for all species. Furthermore, reactive transport in heterogeneous porous media may be efficiently solved in a Lagrangian framework utilizing the approach of Cvetković and Dagan (1994a, b), where advection is solved with particle tracking, while the reactive part is solved in the t-τ domain from the 1-D coupled system of equations as in the Eulerian case. The advantage of this approach lies in adopting efficient particle-tracking for advection and reducing the reactive 3-D problem in Eulerian coordinates to only 1-D in Lagrangian coordinates, where AFCM efficiently tracks all species fronts and significantly compresses the number of collocation points on the adaptive grid.

4.4.4 Density-driven flow and multiphase flow

As for reactive transport, paper I presented the AFCM (also see Kozulić et al, 2007) as a very efficient methodology for density-driven flow (see Gotovac et al., 2003) and multiphase flow (see Gotovac et al., 2005). However, all mentioned papers considered homogeneous media. The real challenge and a question that remains open for density-driven problems is the consideration of heterogeneity effects on seawater intrusion stable problems (such as the Henry problem) related to the width of the transition zone, salt and freshwater fluxes and seawater boundary conditions (Diersch and Kolditz, 2002). Of particular interest is the consideration of instability problems such as the Elder problem (Elder, 1966; Souza and Voss, 1987), in which heterogeneity is a key factor for the onset of instabilities and development of fingers (e.g., Simmons et al., 2001). These instability problems require more powerful, modern computational methodologies, but they also require new physical formulations other than the classic ADE equation. On the other hand, there have recently been many successful implementations of multi-scale finite element methods to multiphase flow problems in heterogeneous porous media (e.g., Enquist et al., 2003), especially in oil and gas problems where the central variable of interest is a quantity of oil and water in a production well.

4.4.5 Transport theories

Different conceptual strategies (as an extension of classic Fickian transport and ADE) for modeling transport in heterogeneous porous media have been presented in the literature, such as the trajectory approach (Dagan, 1984; Cvetković and Dagan, 1994a, b), fractional diffusion equation (Benson et al., 2000), non-local transport approaches (Cushman and Ginn, 1993; Neuman and Orr, 1993) and continuous random-walk methods (Scher et al., 2002, Berkowitz et al., 2002). Very often, the lack of real field experiments leads to the development of many theories that try to explain transport phenomena in a relatively simple way using the sparse available input data. Thus, the presented methodology offers the ability to produce many synthetic simulations for verification of the mentioned theories and bridges the gap between these theories and real applications.

In spite of these theoretical advances, our main problem is still the understanding of the flow velocity and its Lagrangian variants (such as slowness), their transport variables and consequently their relationship with the statistics of hydraulic conductivity.

4.4.6 Risk assessment

Many recent environmental regulatory initiatives stipulate that in order to improve risk characterization, ecological risk analysis needs to identify and conduct the probabilistic risk assessment. The potential toxicity of contaminated groundwater and the associated health risks depend directly on exposure parameters, contaminant concentration and/or solute flux values (Andričević and Cvetković, 1996; Maxwell et al., 1999; Andričević, 2008). It is recognized that high concentration values, along with duration and frequency of appearance, are responsible for severe health risks and need to be predicted probabilistically. The fundamental concept in all methods used in probabilistic risk assess-

ment consists of estimating the exposure concentration distribution and confront it (using different methods) to the distribution of effects obtained from the eco-toxicological studies. For example, a new quantitative microbial risk assessment formulation considering the entire chain of events, from pathogen introduction into the source, their migration through the aquifer pathway, to ingestion at the receptor, and finally the potential infection in the human host (Molin and Cvetković, 2009; Molin et al., 2009). The description of magnitude and temporal distribution of pathogen exposure resulting from relevant hazardous events will benefit from the exhaustive description of the pdf of concentration or solute flux realized through this methodology, in conjunction with the maximum entropy principle. In particular, risk assessment of aquifers with high affinity for formation of preferential flow (e.g. highly heterogeneous), where large fraction of the introduced pathogens exhibit early arrival times, the contribution of the presented methods will prove particularly valuable.

5 CONCLUSIONS

This thesis developed an adaptive Fup multi-resolution approach for solving the flow and transport problems in heterogeneous porous media. The application of this methodology is presented for the multi-resolution description of solutions with sharp fronts as well as for flow and advective transport in highly heterogeneous porous media under mean uniform flow conditions. The main conclusions are summarized as follows:

- The methodology is based on Fup basis functions with compact support, which allows for the construction of different mesh-free and other promising concepts which can work with numerical as well as stochastic methods.
- All flow and transport variables as well as ensemble statistics are described using a multi-resolution representation in the form of linear combinations of Fup basis functions utilizing different Fup transformations. These transformations support a well-known wavelet type of multi-resolution analysis, resolving locations and frequencies at all spatial and/or temporal scales.
- Fup transformations are particularly efficient for the description of heterogeneity and the log-conductivity field, enabling an analysis of different scales and their contribution to flow and transport ensemble statistics.
- The main characteristic of this methodology is a simple and efficient computational procedure that only adds Fup basis functions with the appropriate length of compact support in order to accurately describe solutions on a particular adaptive grid with a prescribed threshold.
- Paper I presented the AFCM, which utilizes the well-known method of lines such that Fup transformations are used for spatial adaptive approximations, while high-order time integration schemes track the solution through the spatial lines. This is particularly important for efficient modeling of density-driven and multi-phase flow as well as reactive transport.
- Each variable is characterized on a particular adaptive grid, which not only results in the computationally more efficient algorithm, but also describes subsurface processes closely related to their understood physical meaning. The methodology inherently yields continuous velocity fields, which are important for accurate transport analysis.
- Paper II presented the improved Monte-Carlo methodology AFMCM for advective transport in multi-Gaussian heterogeneous fields combining a chain of methods for analysis of heterogeneity, flow, transport and MC ensemble statistics. Accuracy and efficiency of this methodology enables the consideration of high heterogeneity effects on flow and travel time statistics (paper III and IV).
- Accuracy and convergence analysis indicated that resolutions $n_Y=8$ and $n_h=32$ yield quite accurate flow solutions and around 4,000 particles enabled reliable travel time statistics. First order theory is robust and accurate for low heterogeneity and partially so for mild heterogeneity.

All necessary flow and transport variables require up to 500 Monte-Carlo realizations in order to stabilize fluctuations of the ensemble statistics in highly heterogeneous formations with $\sigma_Y^2 \leq 8$.

- The Lagrangian and Eulerian velocity statistics and correlation functions diverge for increasing σ_Y^2 due to preferential flow, with the pdf of Lagrangian velocity shifted to higher values and an increasing/more persistent correlation. Both pdfs are strongly non-log-normal for high heterogeneity, while the asymptotic Lagrangian velocity pdf is equal as a flux-averaged Eulerian velocity distribution.
- The transverse displacement is non-Gaussian for all σ_Y^2 and control planes close to the injection source line, with a higher proportion of zero values. However, the distribution converges to a Gaussian distribution even for high σ_Y^2 after x/I_Y=20 because kurtosis consequently goes to three.
- Comparison of the experimental travel time pdf with the inverse Gaussian pdf (ADE solution) in a semi-infinite domain as well as with the log-normal distribution shows that transport in highly heterogeneous porous media may deviate from these models for the first $40(100)I_Y$, in particular regarding the early arrivals. Under these conditions, the first two moments are insufficient for a complete description of travel time arrivals, peak and tailings.
- Paper V presented the inexact Fup maximum entropy algorithm (IFMEA), which efficiently solves the classic maximum entropy moment problem by direct connection of the Fup basis functions and polynomials. The algorithm was applied to the travel time pdf, which demonstrated the significance of the higher moments in its complete characterization (paper IV).
- All travel time moments become linear after certain distance from the source. Initial nonlinearity is caused mainly by the resident injection mode and injection of mass into the zones with low velocity.
- The number of moments needed for an accurate description of the travel time pdf mainly depends on the heterogeneity level. Mean and variance completely describe the travel time pdf for σ_Y^2<3, skewness is dominant for σ_Y^2=4, and kurtosis and the fifth moment are needed for σ_Y^2=6 and 8.
- The highest uncertainty is seen for the early arrivals because they require more moments than other parts of the travel time pdf. In particular, quantitative analysis between the first arrivals for crossing 10^{-4} of the total injected mass predicted by MaxEnt and AFMCM pdf showed that four moments quite accurately describe the first arrivals, which are a key factor for risk assessment.
- Correlation of slowness decreases with increasing σ_Y^2, implying that after $60I_Y$, travel time variance becomes linear and reaches the asymptotic longitudinal dispersion estimated by Eq. (43). Correlation of slope exhibits a "hole effect" with integral scale converging to zero, which appears that the asymptotic transverse dispersion converges to zero as predicted by de Dreuzy et al. (2007).
- In the limit, advective transport in multi-Gaussian heterogeneity structures converges to Fickian transport.

6 FUTURE DIRECTIONS

The capabilities of the presented multi-resolution approach and the quality of obtained results discussed in this thesis open new questions and possibilities for future work:

- Application of other atomic basis functions, not only those necessary in subsurface modeling.
- Extension of the presented methodology to 3-D flow and transport problems using massive parallel processing.
- Improvement to the flow solver, the most demanding AFMCM step, by: a) exponential atomic basis functions defining the relationship between frequencies of these basis functions and properties of the heterogeneous log-conductivity field and b) new stochastic methods that directly solve ensemble statistics (pdf and related moments).
- A new stochastic approach may be found as an extension of the IFMEA to the multivariate pdf, thus combining the multi-resolution nature of Fup basis functions and the versatility of the BME approach (Christakos, 2000) for real applications.
- Flow and travel time statistics in non-Gaussian heterogeneity structures (related to Zinn and Harvey, 2003).
- Influence of the pore-scale dispersion on concentration and solute flux pdf and related, possibly higher, moments (Andričević, 2008).
- Reactive transport simulations using the approach of Cvetković and Dagan (1994a, b), where advection is solved with particle tracking, while the reactive part is solved in the t-τ domain from the 1-D coupled system of advection-reaction equations.
- Density-driven flow in heterogeneous porous media and find out relationship between lnK variance and correlation length on the one side and physical parameters that govern the onset of instabilities and existence of fingers on the other side.

7 REFERENCES

Aarnes JE. 2004. On the use of a mixed multiscale finite element method for greater flexibility and increased speed or improved accuracy in reservoir simulation. *SIAM Multiscale Modeling and Simulation*, **2 (3)**: 421–439.

Ababou R, McLaughlin D, Gelhar LW, Thompson AFB. 1989. Numerical simulation of three-dimensional saturated flow in randomly heterogeneous porous media. *Transp. Porous Media*. **4(6)**: 549-566.

Abramov R. 2007. An improved algorithm for the multidimensional moment-constrained maximum entropy problem. *J. Comp. Phys*., **226**: 621–644.

Abramov R. 2009. The multidimensional moment-constrained maximum entropy problem: A BFGS algorithm with constraint scaling. *J. Comp. Phys.*, **228**: 96–108.

Andričević R, Cvetković V. 1996. Evaluation of risk from contaminants migrating by groundwater. *Water Resour. Res.*, **32(3)**: 611-621.

Andričević R, Cvetković V. 1998. Relative dispersion for solute flux in aquifers. *J Fluid Mech.* **361**:145–174.

Andričević R. 2008. Exposure concentration statistics in the subsurface transport. *Water Resour. Res.* **31(8)**: 714-725.

Bakr AA, Gelhar LW, Gutjahr AL, MacMillan JR. 1978. Stochastic analyses of spatial variability in subsurface flows: 1. Comparison of one – and three – dimensional flows. *Water Resour Res.* **14(2)**: 263-272.

Bandyopadhyay K., Bhattacharya A, Biswas P, Drabold D. 2005. Maximum entropy and the problem of moments: A stable algorithm, *Phys. Rev. E,* **71**: 05771.

Bellin A, Salandin P, Rinaldo A. 1992. Simulation of dispersion in heterogeneous porous formations: Statistics, first order theories, convergence of computations. *Water Resour .Res.* **28(9)**: 2211-2227

Bellin A, Rubin Y, Rinaldo A. 1994. Eulerian-Lagrangian approach for modeling of flow and transport in heterogeneous geological formations. *Water Resour. Res.* **30(11)**: 2913-2924.

Bellin A, Rubin Y. 1996. HYDRO_GEN: A spatially distributed random field generator for correlated properties. *Stochastic Hydrol. Hydraul.* **10(4)**: 253-278.

Benke R, Painter S. 2003. Modeling conservative tracer transport in fracture networks with a hybrid approach based on the Boltzmann transport equation, *Water Resour. Res.*, **39(11)**: 1324, doi:10.1029/2003WR001966.

Benson DA, Wheatcraft SW, Meerschaert MM. 2000. The fractional-order governing equation of Levy motion. *Water Resour. Res.* **36***:* 1413–1423.

Berkowitz B, Klafter J, Metzler R, Scher H. 2002. Physical pictures of transport in heterogeneous media: Advection-dispersion, random-walk, and fractional derivative formulations. *Water Resour. Res.* **38(10)**: 1191, doi:10.1029/2001WR001030.

Boggs JM, Young SC, Beard LM, Gelhar LW, Rehfeldt KR, Adams EE. 1992. Field study of dispersion in a heterogeneous aquifer: 1. Overview and site description. *Water Resour. Res.*, **28(12)**: 3281– 3291.

Cao J, Kitanidis PK. 1999. Adaptive grid-simulation of groundwater flow in heterogeneous aquifers. *Adv Water Resour*; **22(7)**: 681-696.

Christakos G. 2000. *Modern Spatiotemporal Statistics*. Oxford University Press, New York.

Cordes C, Kinzelbach W. 1992. Continuous Groundwater Velocity Fields and Path Lines in Linear, Bilinear, and Trilinear Finite Elements. *Water Resour Res.* **28(11)**: 2903-2911.

Cruz P, Alves MA, Magalhes FD, Mendes. 2003. A. Solution of hyperbolic PDEs using a stable adaptive multiresolution method. *Chemical Engineering Science.* **58**: 1777-1792.

Cushman JH, Ginn TR. 1993. Nonlocal dispersion in media with continuously evolving scales of heterogeneity. *Transp. Porous Media*. **13**: 123-138.

Cvetković V, Shapiro AM, Dagan G. 1992. A solute-flux approach to transport in heterogeneous formations: 2. Uncertainty analysis. *Water Resour Res.* **28(5)**: 1377-1388.

Cvetković V, Dagan G. 1994a . Transport of kinetically sorbing solute by steady random velocity in heterogeneous porous formations. *J. Fluid Mech.* **265**: 189-215.

Cvetković V, Dagan G. 1994b. Reactive transport and immiscible flow in geological media, I. Theory. *Proc. R. Soc. London A*. **452**: 303-328.

Cvetković V, Cheng H, Wen X-H. 1996. Analysis of linear effects on tracer migration in heterogeneous aquifers using Lagrangian travel time statistics. *Water Resour. Res.* **32(6)**: 1671-1670.

Cvetković V, Dagan G, Cheng H. 1998. Contaminat transport in aquifers with spatially variable hydraulic and sorption parameters. Proceedings Royal Soc. London A, 1998.

Cruz P, Alves MA, Magalhes FD, Mendes A. 2003. Solution of hyperbolic PDEs using a stable adaptive multiresolution method. *Chemical Engineering Science*, **58**: 1777-1792.

Dagan G. 1984. Solute transport in heterogeneous porous formations. *J Fluid Mech.* **145**: 151-177.

Dagan G. 1985. Stochastic modeling of groundwater flow by unconditional and conditional probabilities: The inverse problem *Water Resour. Res.* **21(1):** 65-72.

Dagan G. 1987. Theory of solute transport by groundwater Annu. *Rev. Fluid Mech*. **19**: 183-215

Dagan G. 1989. *Flow and Transport in Porous Formations*. Berlin: Springer-Verlag.

Dagan G, Cvetković V, Shapiro AM. 1992. A solute-flux approach to transport in heterogeneous formations: 1. The general framework. *Water Resour Res*. **28(5)**: 1369-1376.

Dagan, G. 1994. The significance of heterogeneity of evolving scales to transport in porous formation. *Water Resour. Res.* **30(12)**: 3327-3336.

Dagan G., Fiori A. 1997. The influence of pore scale dispersion on concentration statistical moments in transport through heterogeneous aquifers, *Water Resour. Res.* **33(7)**: 1595-1605.

de Dreuzy JR, Beaudoin A, Erhel J. 2007. Asymptotic dispersion in 2D heterogeneous porous media determined by parallel numerical simulations. Water Resour Res. **43**: W10439, doi: 10.1029/2006WR005394.

Demmy G, Berglund S, Graham W. 1999. Injection mode implications for solute transport in porous media: Analysis in a stochastic Lagrangian framework. *Water Resour. Res.* **35(7)**: 1965-1974.

Deng FW, Cushman JH. 1995. On higher-order corrections to the flow velocity covariance tensor. *Water Resour. Res.* **31(7)**: 1659-1672.

Destouni G, Graham W. 1995. Solute transport through an integrated heterogeneous soil-groundwater system. *Water Resour. Res.* **31(8)**: 1935-1944.

Deutsch CV, Journel AG. 1998. GSLIB: *A geostatistical software library and user's guide*. Oxford University Press, London

Di Federico V, Neumann SP, 1988. Flow in multiscale log conductivity fields with truncated power variograms. *Water Resour. Res.* **34(5)**: 963-974.

Diersch HJG, Kolditz O. 2002. Variable density flow and transport in porous media: approaches and challenges. *Advances in Water Resources*. **25**: 899-944.

Durlofsky LJ. 1992. Representation of grid block permeability in coarse scale models of randomly heterogeneous porous media. *Water Resour Res.* **28 (7)** : 1791-1800.

Dykaar BB, Kitanidis P.K. 1992. Determination of the effective hydraulic conductivity for heterogeneous porous media using a numerical spectral approach, 1. Method. *Water Resour Res.* **28 (4)**: 1155-1166.

E W, Ming P, Zhang P. 2004. Analysis of the heterogeneous multiscale method for elliptic homogenization problems. *Journal of the American Mathematical Society*, **18(1**): 121-156.

Einstein A. 1905. On the Electrodynamics of Moving Bodies. *Annalen der Physik*, **17**:891 (English translation by W. Perrett and G.B. Jeffery).

Ebrahimi F, Sahimi M. 2002. Multiresolution wavelet coarsening and analysis of transport in heterogeneous media. *Physica A* **316**: 160 – 188.

Elder JW. 1967. Transient convection in a porous medium. *J. Fluid Mech.*, **27**: 609-623.

Enquist B, Lotstedt P, Runborg O. 2003. *Multiscale methods in science and engineering*. Stockholm: Springer-Verlag.

Ezzedine S, Rubin Y. 1996. A Geostatistical Approach to the Conditional Estimation of Spatially Distributed Solute Concentration and Notes on the Use of Tracer Data in the Inverse Problem. *Water Resour. Res.*, **32(4)**: 853-861.

Fiori A, Dagan G. 1999. Concentration Fluctuations in Transport by Groundwater: Comparison Between Theory and Field Experiments. *Water Resour. Res.*, **35(1)**: 105-112.

Fiori A, Dagan G. 2000. Concetration fluctuations in aquifer transport: A rigorous first-order solution and application. *J. Contam. Hydrol.* **45**: 139 – 163.

Fiori A, Berglund S, Cvetković V, Dagan G, 2002. A first-order analysis of solute flux statistics in aquifers: The combined effect of pore-scale dispersion, sampling, and linear sorption kinetics *Water Resour. Res.* **38(8)**: 10.1029/2001WR000678

Fiori A., Janković I, Dagan G. 2006. Modeling flow and transport in highly heterogeneous three-dimensional aquifers: Ergodicity, Gaussianity, and anomalous behavior—2. Approximate semianalytical solution. *Water Resour. Res.* **42**: W06D13, doi:10.1029/2005WR004752.

Gelhar LW, Axness CL. 1983. Three-dimensional stochastic analysis of macrodispersion in aquifers. *Water Resour. Res.* **19(1)**: 161-180.

Gelhar LW. 1993. *Stochastic Subsurface Hydrology*. NJ: Prentice Hall, Englewood Cliffs.

Gomez-Hernandez JJ, WenX-H. 1998. To be or not to be multi- Gaussian? A reflection on stochastic hydrogeology, *Adv. Water Resour.* **21**: 47-61.

Gotovac B. 1986. Numerical modeling of engineering problems with help of smooth finite basis functions (in Croatian), Department of Civil Engineering, University of Zagreb, Zagreb.

Gotovac, B, V. Kozulić 1999. On a selection of basis functions in numerical analyses of engineering problems. *Int J Eng Model.* **12(1-4)**: 25-41.

Gotovac B, Kozulić V. 2002. Numerical solving the initial value problems by R_{bf} basis functions. *Structural Engineering & Mechanics*. **14(3)**: 263-285.

Gotovac H, Andričević R, Gotovac B, Kozulić V, Vranjes M. 2003. An improved collocation method for solving the Henry problem. *Journal of Contaminant Hydrology*. **64**:129-149.

Gotovac H, Andričević R, Vranješ M, Radelja T. 2005. Multilevel adaptive modeling of multiphase flow in porous media, Proceedings of The Computational Methods in Multiphase Flow III, Portland, Maine, USA, November 2-5.

Graham W, McLauglin D. 1989a, Stochastic analysis of nonstationary subsurface solute transport, 1. Unconditional moments. *Water Resour. Res.* **25(2)**: 215-232.

Graham W, McLauglin D. 1989b, Stochastic analysis of nonstationary subsurface solute transport, 2. Conditional moments. *Water Resour. Res.* **25(11)**: 2332-2335.

Guadagnini A, Sanchez-Villa X, Riva M, De Simoni M. 2003. Mean travel time of conservative solutes in randomly unbounded domains under mean uniform flow. *Water Resour. Res.*, **30(3)**: 1050, doi:10.1029/2002WR001811.

Harvey C, Gorelick S. 2000. Rate-Limited Mass Transfer or Macrodispersion: Which Dominates Plume Evolution at the Macrodispersion Experiment (MADE) Site?. *Water Resour. Res.*, **36(3)**: 637-650.

Hassan AE, Cushman JH, Delleur JW. 1998. A Monte-Carlo assessment of Eulerian flow and transport perturbation models. *Water Resour Res.* **34(5)**: 1143-1163.

Hassan AE, Andričević R, Cvetković V. 2001. Computational issues in the determination of solute discharge moments and implications or comparison to analytical solutions. *Adv. Water Resour.* **24**: 617-619.

He X, Ren L. 2005. Finite volume multiscale finite element method for solving the groundwater flow problems in heterogeneous porous media. *Water Resour. Res.*, **41**, W10417, doi:10.1029/2004WR003934.

Helmig R. 1998. *Multiphase flow and transport processes in the subsurface.* Berlin: Springer. p. 367.

Hou TY, Wu X-H. 1997. A multiscale finite element method for elliptic problems in composite materials and porous media*, J Comput Phys.* **134**: 169-189.

Hou, TY, Wu X-H, Cai Z. 1999. Convergence of a multiscale finite element method for elliptic problems with rapidly oscillating coefficients. *Math. Comp.*, **68**: 913-943.

Hsu KC, Zhang D, Neuman SP. 1996. Higher-order effects on flow and transport in randomly heterogeneous porous media. *Water Resour Res.* **32(3)**: 571-582.

Hsu KC, Lamb Y. 2000. On the second order correction to velocity covariance for 2D statistically isotropic porous media, *Water Resour. Res.* **36(1)**: 349-354

Hsu KC. 2003. The influence of the log-conductivity autocovariance structure on macrodispersion coefficients. *J Contam Hydrol* . **65**: 65 – 77.

Janković I, Barnes R. 1999. Three-dimensional flow through large numbers of spherical inhomogeneities. *J. Hydrol.*, **226**: 224–233.

Janković I, Fiori A, Dagan G. 2003. Flow and transport in highly heterogeneous formations: 3. Numerical simulation and comparison with theoretical results. *Water Resour Res.* **9(9)**: 1270, doi:10.1029/2002WR001721.

Janković I., Fiori A, Dagan G. 2006. Modeling flow and transport in highly heterogeneous three-dimensional aquifers: Ergodicity, Gaussianity, and anomalous behavior—1. Conceptual issues and numerical simulations. *Water Resour Res.* **42**: W06D12, doi:10.1029/2005WR004734.

Janković I, Stewart DR, Barnes RJ, Dagan G. 2009. Is Transverse Macrodispersivity in Three-dimensional Groundwater Transport Equal to Zero? A Counterexample. *Water Resour Res.*, in review.

Jaynes ET. 1957. Information theory and statistical mechanics. *Phy. Rev.* **106**: 620-630

Jenny P, Lee SH, Tchelepi HA. 2003. Multi-scale finite-volume method for elliptic problems in subsurface flow simulation, *J. Comp. Phys.*, **187(1)**: 47-67.

Kansa EJ. 1990. Multiquadratics – a scattered data approximation scheme for applications to computational fluid-dynamics. 1. Surface approximations and partial derivative estimates. *Computers and Mathematics with Applications.* **19(8-9)**: 127-145.

Kapoor V, Gelhar W. 1994. Transport in three-dimensional heterogeneous aquifers. 1. Dynamics of concentration fluctuation. *Water Resour. Res.* **50(6)**: 1775-1788.

Kinzelbach W. 1988. The random walk method in pollutant transport simulation. in Groundwater flow and Quality Modelling, NATO ASI Ser., Ser. C Math and Phys. Sci., vol. 224, edited by E. Custidio, A. Gurgui, and J.P. Lobo Ferreria, pp. 227-246.

Kitanidis PK. 1990. Effective hydraulic conductivity for gradually-varying flow. *Water Resour Res.* **26 (6)** : 1197-1208.

Kitanidis PK. 1994. The concept of the dilution index *Water Resour. Res.* **30(7)**: 2011-2026.

Kitanidis PK. 1997. *Introduction to Geostatistics: Applications in Hydrogeology*, Cambridge University Press, Cambridge.

Knudby C, Carrera J. 2005. On the relationship between indicators of geostatistical, flow and transport connectivity. *Adv. Water Resour.* **28**: 405-421.

Kozulić V, Gotovac B. 2000. Numerical analysis of 2-D problems using Fup basis functions. *Int J Eng Mod.* **13 (1-2)**: 7-18.

Kozulić V, Gotovac H, Gotovac B. 2007. An Adaptive Multi-resolution Method for Solving PDE's. *Computers, Materials and Continua*, 6(2): 51-70.

Kreft A, Zuber A. 1978. On the physical meaning of the dispersion equation and its solution for different initial and boundary conditions. *Chem. Eng. Sci.* **33**: 1471-1480

Kolodiazhny VM, Rvachev VA. 2007. Atomic functions: Generalization to the multivariable case and promising applications. *Cybernetics and Systems Analysis.* **43 (6)**: 893–911.

Kolovos A, Christakos G, Serre ML, Miller CT. 2002. Computational Bayesian maximum entropy solution of a stochastic advection-reaction equation in the light of site-specific information, *Water Resour. Res.*, **38 (12)**: 1318, doi:10.1029/2001WR000743.

Kurganov A, Tadmor E. 2000. New high resolution central scheme for nonlinear conservation laws and convection-diffusion equations. *J. of Comp. Phys.,*. **160**: 241-282.

Kravchenko VF, Rvachev VA, Rvachev VL. 1995. Mathematical methods for signal processing on the basis of atomic functions (Russian). *Radiotekhnika i Elektronika*, **40(9)**: 1385-1406.

LaBolle EM, Fogg GE, Thompson AFB. 1996. Random walk simulation of transport in heterogeneous porous media: Local mass-conservation problem and implementation methods. *Water Resour Res.* **32(3)**: 583-593.

LeBlanc D, Garabedian S, Hess K, Gelhar L, Quadri R., Stollenwerk K, Wood W. 1991. Large-Scale Natural Gradient Tracer Test in Sand and Gravel, Cape Cod, Massachusetts 1. Experimental Design and Observed Tracer Movement. *Water Resour. Res.* **27(5)**: 895-910.

Le Borgne T, de Dreuzy J-R, Davy P, Bour O. 2007. Characterization of the velocity field organization in heterogeneous media by conditional correlation, *Water Resour. Res.*, **43**: W02419, doi:10.1029/2006WR004875.

Le Borgne T, Dentz M, Carrera J. 2008. Lagrangian Statistical Model for Transport in Highly Heterogeneous Velocity Fields. *Phys. Rev. Lett.*, **101**: 090601.

Li H, Zhang D. 2007. Probabilistic collocation method for flow in porous media: Comparisons with other stochastic method. ***Water Resour. Res.***, **43**: Doi: 10.1029/2006WR005673.

Li H, Zhang D. 2007. Probabilistic collocation method for flow in porous media: Comparisons with other stochastic method. ***Water Resour. Res.***, **43**: Doi: 10.1029/2006WR005673.

Lin G, Tartakovsky AM. 2009. An efficient, high-order probabilistic collocation method on parse grids for three-dimensional flow and solute transport in randomly heterogeneous porous media. Adv. *Water Resour.,*. **32(5)**: 712-722.

Mackay DM, Freyberg DL, Roberts PV. 1986. A natural gradient experiment on solute transport in a sand aquifer, 1. Approach and overview of plume movement. *Wat. Resour. Res.* **22(13)**: 2017-2029.

Mallat SG. 1989. A Theory for Multi-Resolution Signal Decomposition: The Wavelet Representation. *IEEE Transactions on Pattern Analysis and Machine Intelligence.* **2(7)**: 674-693.

Maxwell R, Kastenberg WE. 1999. Stochastic environmental risk analysis: An integrated methodology for predicting cancer risk from contaminated groundwater. *Stochastic Environ. Res.* **34849**: 833-847.

McDonald MG, Harbaugh AW. 1988. A modular three-dimensional finite-difference groundwater flow model, Techniques of water resource investigations, **06**-A1, USGS.

Mead L., Papanicolaou N. 1984. Maximum entropy in the problem of moments. *J. Math. Phys.,* **25**: 2404–2417.

Molin S, Cvetković V. 2009. Quantitative Microbial Risk Assessment in heterogeneous aquifers: 1. The barrier function. *Water Resour. Res.,* in review.

Molin S, Cvetković V, Stenstrom TA. 2009. Quantitative Microbial Risk Assessment in heterogeneous aquifers: 2. Infection risk sensitivity. *Water Resour. Res.,* in review.

Moreno L, Tsang CF. 1994. Flow channeling in strongly heterogeneous porous media. A numerical study. *Water Resour. Res.,* **30(5)**: 1421-1430.

Mose R, Siegel P, Ackerer P. 1994. Application of the mixed hybrid finite element approximation in a groundwater model: Luxury or necessity? *Water Resour Res.*, **30**: 3001-3012.

Neuman, S.P. and S. Orr (1993), Prediction of steady state flow in nonuniform geologic media by conditional moments: Exact nonlocal formalism, effective conductivity, and weak approximation. *Water Resour. Res.* **29(2)**: 341-364.

Neuman SP, Zhang YK. 1990. A quasi-linear theory of non-Fickian and Fickian subsurface dispersion: 1. Theoretical analysis with application to isotropic media. *Water Resour Res.,* **26**: 867-902.

Rubin Y. 1990. Stochastic modeling of macrodispersion in heterogeneous porous media. *Water Resour Res.,* **26(1)**: 133-141 (with correction in Water Resour Res 1990; 26(10): 2631).

Rubin Y, Dagan G. 1992. Conditional estimation of solute travel time in heterogeneous formations: Impact of transmissivity measurements. *Water Resour Res.* **28(4)**: 1033-1040.

Rubin Y. 2003. *Applied Stochastic Hydrogeology*. N.Y: Oxford University Press; 391. p.

Rvachev VL, Rvachev VA. 1971. Pro odnu finitnu funkciju. *DAN URSR. Ser. A (in Russian.,* **6**: 705-707.

Rvachev VL. 1982. *Teorija R-funkcij i nekotorija jeje priloženija (in Russian)*. Kiev: Naukova dumka. p. 551.

Rvachev VL, Sheiko TI, Shapiro V, Tsukanov I. 2000. On completeness of RFM solution structures. *Computational Mechanics*, **25**: 305–316.

Salandin P, Fiorotto V. 1998. Solute transport in highly heterogeneous aquifers. *Water Resour Res.,* **34(5)**: 949-961.

Scher H, Margolin G, Berkowitz B. 2002. Towards a unified framework for anomalous transport in heterogeneous media. *Chemical Physics.*, **284**: 349-359.

Selros JO, Cvetković V. 1992. Modeling Solute advection Coupled With Sorption Kinetics in Heterogeneous Formations. *Water Resour. Res.,* **28(5)**: 1271-1278

Selros JO. 1995. Temporal moments for nonergodic solute transport in heterogeneous aquifers. *Water Resour. Res.,* **31(7)**: 1705-1712

Serre ML, Christakos G, Li H, Miller CT. 2003. A BME solution to the inverse problem for saturated groundwater flow. *Stochastic Environ. Res. Risk Assess.,* **17**: 354– 369.

Shannon CE. 1948. The Mathematical Theory of Communication, *Bell System Tech. J.,* **27**: 379-423.

Shapiro A, Cvetković V. 1988. Stochastic Analysis of Solute Arrival Time in Heterogeneous Porous Media, *Water Resour. Res.*, **24(10)**: 1711-1718.

Shi L, Zhang D, Lin L, Yang J, Li H. 2009. A Multiscale Probabilistic Collocation Method for Subsurface Flow in Heterogeneous Media. *Water Resour. Res.,* in review.

Simmons CT, Fenstemaker TR, Sharp JM. 2001. Variable-density groundwater flow and solute transport in heterogeneous media: approaches, resolutions and future challenges. *J. Contam. Hydrol.* **52(1-4)**: 245-75.

Strack ODL. 1989, *Groundwater Mechanics*. Prentice-Hall, Upper Saddle River, N. J.

Taylor GI. 1921. Diffusion by continuous movements. *Proc London Math Soc.* **20**: 196-212.

Thompson AFB, Gelhar LW. 1990. Numerical simulation of solute transport in three-dimensional, randomly heterogeneous porous media. *Water Resour Res.* **126(10)**: 2541-2562.

Tsukanov I, Shapiro V. 2005. Meshfree modeling and analysis of physical fields in heterogeneous media. *Advances in Computational Mathematics*, **23(1–2)**: 95–124.

Turek I. 1988. A maximum-entropy approach to the density of states with the recursion method, *J. Phys. C.*, **21**: 3251–3260.

Van Lent T, Kitanidis PK. 1996. Effects of first order approximations on head and specific discharge covariances in high-contrast log-conductivity. *Water Resour Res.* **32(5)**: 1197-1297.

Vasilyev OV, Bowman CS. 2000. Second Generation wavelet collocation method for the solution of the partial differential equations. *J. Comp. Phys.* **165**: 660-693.

Vasilyev OV, Kevlahan NKR. 2005. An adaptive multilevel wavelet collocation method for elliptic problems. *J. Comp. Phys.* **206**: 412-431.

Verner JH.1978. Explicit Runge-Kutta methods with estimates of the local truncation error, SIAM *J. Numer. Anal.*. **15**: 772-790.

Voss CI. 1984. A finite-element simulation model for saturated-unsaturated fluid-density-dependent groundwater flow with energy transport or chemically-reactive single-species solute transport. *U.S. Geol. Surv. Water Resour. Invest.* p. **409** [Rep 84-4369].

Voss CI, Souza WR. 1987. Variable density flow and solute transport simulation of regional aquifers containing a narrow freshwater-saltwater transition zone. *Water Resour. Res.* **26**: 2097-2106.

Wen X-H, Gomez-Hernandez JJ. 1998. Numerical modeling of macrodispersion in heterogeneous media: a comparison of multi-Gaussian and non-multi-Gaussian models. *J. Contam. Hydrol.*. **30**: 129-156.

Zegeling PA, Werver JG, van Eijkeren JKM. 1992. Application of moving grid method to a class of 1-D brine transport problems. *International Journal of Numerical Methods in Fluids*, **15(2)**: 175-191.

Zhang D. 2002. *Stochastic Methods for Flow in Porous Media: Copying With Uncertainties.* Academic Press, San Diego.

Zhang D, Lu Z. 2004. An efficient, high-order perturbation approach for flow in random porous media via Karhunen-Loeve and polynomial expansions. *J. Comp. Phys.*, **194(2)**: 773-794.

Zinn B, Harvey CF. 2003. When good statistical models of aquifer heterogeneity go bad: A comparison of flow, dispersion, and mass transfer in connected and multivariate Gaussian hydraulic conductivity fields. *Water Resour. Res.* **39 (3)**: 1051, doi:10.1029/2001WR001146.